Macrophage polarization is linked to Ca^{2+}-independent phospholipase $A_2\beta$-derived lipids and cross-cell signaling in mice

Alexander J. Nelson,[1,*,†] Daniel J. Stephenson,[1,§] Christopher L. Cardona,[§] Xiaoyong Lei,[*,†] Abdulaziz Almutairi,[*,†] Tayleur D. White,[*,†] Ying G. Tusing,[*,†] Margaret A. Park,[§] Suzanne E. Barbour,[**] Charles E. Chalfant,[2,§,††] and Sasanka Ramanadham[2,3,*,†]

Department of Cell, Developmental, and Integrative Biology* and Comprehensive Diabetes Center,[†] University of Alabama at Birmingham, Birmingham, AL 35294; Department of Cell Biology, Microbiology, and Molecular Biology (CMMB),[§] University of South Florida, Tampa, FL 33620; Department of Biochemistry and Molecular Biology,[**] University of Georgia, Athens, GA 30602; and Research Service,[††] James A. Haley Veterans Hospital, Tampa, FL 33612

ORCID ID: 0000-0002-1664-0657 (S.R.)

Abstract **Phospholipases A_2 (PLA_2s) catalyze hydrolysis of the *sn*-2 substituent from glycerophospholipids to yield a free fatty acid (i.e., arachidonic acid), which can be metabolized to pro- or anti-inflammatory eicosanoids. Macrophages modulate inflammatory responses and are affected by Ca^{2+}-independent phospholipase A_2 (PLA_2)β ($iPLA_2\beta$). Here, we assessed the link between $iPLA_2\beta$-derived lipids (iDLs) and macrophage polarization. Macrophages from WT and KO (*$iPLA_2\beta^{-/-}$*) mice were classically M1 pro-inflammatory phenotype activated or alternatively M2 anti-inflammatory phenotype activated, and eicosanoid production was determined by ultra-performance LC ESI-MS/MS. As a genotypic control, we performed similar analyses on macrophages from *RIP.$iPLA_2\beta$.Tg* mice with selective $iPLA_2\beta$ overexpression in β-cells. Compared with WT, generation of select pro-inflammatory prostaglandins (PGs) was lower in *$iPLA_2\beta^{-/-}$*, and that of a specialized pro-resolving lipid mediator (SPM), resolvin D2, was higher; both changes are consistent with the M2 phenotype. Conversely, macrophages from *RIP.$iPLA_2\beta$.Tg* mice exhibited an opposite landscape, one associated with the M1 phenotype: namely, increased production of pro-inflammatory eicosanoids (6-keto $PGF_1\alpha$, PGE_2, leukotriene B_4) and decreased ability to generate resolvin D2. These changes were not linked with secretory PLA_2 or cytosolic $PLA_2\alpha$ or with leakage of the transgene. Thus, we report previously unidentified links between select $iPLA_2\beta$-derived eicosanoids, an SPM, and macrophage polarization. Importantly, our findings reveal for the first time that β-cell $iPLA_2\beta$-derived signaling can predispose macrophage responses. These findings suggest that iDLs play critical roles in macrophage polarization, and we posit that they could be targeted therapeutically to counter inflammation-based disorders.—** Nelson, A. J., D. J. Stephenson, C. L. Cardona, X. Lei, A. Almutairi, T. D. White, Y. G. Tusing, M. A. Park, S. E. Barbour, C. E. Chalfant, and S. Ramanadham. **Macrophage polarization is linked to Ca^{2+}-independent phospholipase $A_2\beta$-derived lipids and cross-cell signaling in mice. *J. Lipid Res.* 2020.** 61: **143–158.**

Supplementary key words inflammation • macrophage phenotype • lipidomics • eicosanoids • resolvin D2 • intercellular signaling

This work was supported by funding from: the University of Alabama at Birmingham Department of Cell, Developmental, and Integrative Biology; the Iacocca Family Foundation, the King Saud bin Abdulaziz University for Health Sciences, Riyadh, Saudi Arabia (A.A.); Veterans Administration Grants BX001792 (C.E.C.) and 13F-RCS-002 (C.E.C.); National Institutes of Health Grants R01 DK69455 (S.R.), R01 DK110292 (S.R.), Diversity Research Supplement (T.D.W.), R01 HL125353 (C.E.C.), U01 HD087198 (C.E.C.), RR031535 (C.E.C.), and R01 AI139072 (C.E.C.); and University of South Florida funds [initiative 0131845 (M.A.P.)]. The content is solely the responsibility of the authors and does not necessarily represent the official views of the National Institutes of Health. The authors declare that they have no conflicts of interest with the contents of this article.

Manuscript received 23 July 2019 and in revised form 27 November 2019.

Published, JLR Papers in Press, December 9, 2019
DOI https://doi.org/10.1194/jlr.RA119000281

This article is available online at https://www.jlr.org

Abbreviations: AA, arachidonic acid; *Arg2*, arginase 2; COX, cyclooxygenase; $cPLA_2$, cytosolic phospholipase A_2; DHET, dihydroxyeicosatrienoic acid; DHGLA, dihomo-γ-linolenic acid; EET, epoxyeicosatrienoic acid; *Fabpi*, fatty acid-binding protein, intestinal; GSIS, glucose-stimulated insulin secretion; iDL, Ca^{2+}-independent phospholipase $A_2\beta$-derived lipid; IFNγ, interferon-γ; IL, interleukin; $iPLA_2\beta$, Ca^{2+}-independent phospholipase $A_2\beta$; LO, lipoxygenase; LPS, lipopolysaccharide; LT, leukotriene; *Mrc1*, mannose receptor C type 1; $M\Phi_{KO}$, macrophages isolated from KO (*$iPLA_2\beta^{-/-}$*) mice; $M\Phi_{Tg}$, macrophages isolated from transgenic (*RIP.$iPLA_2\beta$.Tg*) mice; $M\Phi_{WT}$, macrophages isolated from WT mice; NOD, nonobese diabetic; PLA_2, phospholipase A_2; PG, prostaglandin; RIP, rat insulin promoter; qPCR, quantitative PCR; $sPLA_2$, secretory phospholipase A_2; SPM, specialized pro-resolving lipid mediator; Tg, transgenic; TXB_2, thromboxane B_2; UPLC ESI-MS/MS, ultra-performance LC ESI-MS/MS.

[1] A. J. Nelson and D. J. Stephenson contributed equally to this work.
[2] C. E. Chalfont and S. Ramanadham contributed equally to this work.
[3] To whom correspondence should be addressed.
e-mail: sramvem@uab.edu
S The online version of this article (available at https://www.jlr.org) contains a supplement.

T1D is a consequence of autoimmune destruction of β-cells, involving activation of cellular immunity and inflammation that lead to infiltration of islets by leukocytes (1). Lipid signaling is recognized as a key modulator of inflammation and immune responses (2). For instance, arachidonic acid (AA) and oxidized lipids [i.e., prostaglandins (PGs) and leukotrienes (LTs)] (3) generated via its metabolism can trigger immune responses leading to β-cell death (4, 5). They are generated via cyclooxygenases (COXs) and lipoxygenases (LOs), subsequent to phospholipase A_2 (PLA_2)-mediated hydrolysis of AA (6–12) from membrane glycerophospholipids.

Among the family of PLA_2s is the Ca^{2+}-independent phospholipase $A_2\beta$ ($iPLA_2\beta$), and its activity promotes deleterious outcomes in experimental and clinical diabetes (13–15). Immune cells express $iPLA_2\beta$ (16–20) and inhibition of $iPLA_2\beta$ reduces generation of reactive oxygen species (18) and antibody production from B-cells and TNFα from $CD4^+$ T-cells (20) and macrophages (21). TNFα acts as a powerful chemoattractant (22) and is produced by $CD4^+$ T-cells within inflamed islets during diabetes development (23). TNFα overexpression exacerbates insulitis while the opposite occurs in TNFα-receptor-null mice (24). In this regard, lipids derived from $iPLA_2\beta$ activation, but not other PLA_2s, promote monocyte chemotaxis (18, 21, 25, 26) and provide migratory directionality to monocytes to inflamed sites (27). Inhibition of $iPLA_2\beta$ has shown to be effective against diseases related to autoimmunity (28) and inflammation (29–32).

Macrophages are important for innate and adaptive immunity and participate in autoimmune-mediated destruction of β-cells and T1D. In diabetes-prone individuals, immune cells, including macrophages, migrate to pancreatic islets and secrete pro-inflammatory cytokines and reactive oxygen species that result in β-cell death (33). Two different activation states of macrophages have been described; M1 pro-inflammatory macrophages (34), which are classically activated by interferon-γ (IFNγ), lipopolysaccharide (LPS), or TNFα, and M2 macrophages, which are alternatively activated by interleukin (IL)-4 or IL-10 (35). Whereas M1 macrophages are recognized causative factors in T1D development (36), M2 macrophages protect against T1D (37). Pro-inflammatory eicosanoids have been linked to macrophage phagocytosis, adhesion, and apoptosis, and amplifying macrophage-derived eicosanoid release (38–41).

Macrophages express $iPLA_2\beta$ (18, 42), and our recent studies reveal that activation of $iPLA_2\beta$ promotes macrophage polarization toward the M1 inflammatory phenotype (42). In contrast, $iPLA_2\beta$ deficiency favors macrophage polarization toward the M2 anti-inflammatory phenotype. Further, inhibitors of $iPLA_2\beta$, COX, and 12-LO reduce M1 inflammatory markers, recapitulating the $iPLA_2\beta^{-/-}$ macrophage phenotype. Collectively, these findings suggest that $iPLA_2\beta$-derived lipids (iDLs) modulate immune responses.

Given the importance of macrophages to T1D development and evidence for a role of $iPLA_2\beta$ in modulating macrophage polarization and function, we sought to identify iDLs generated by activated macrophages, which could be targeted to counter autoimmune/inflammatory-based disorders. To facilitate our assessments, we utilized targeted/quantitative MS analyses of eicosanoids produced by macrophages isolated from WT ($M\Phi_{WT}$) and $iPLA_2\beta^{-/-}$ (KO, $M\Phi_{KO}$) mice. As a control for the genotype, we performed similar analyses with macrophages isolated from *RIP.iPLA$_2\beta$.Tg* [transgenic (Tg), $M\Phi_{Tg}$] mice, which selectively overexpress $iPLA_2\beta$ in β-cells (43, 44).

We found that $iPLA_2\beta$ deficiency led to an attenuated pro-inflammatory and amplified anti-inflammatory lipid profile that was consistent with a macrophage M2 phenotype. In contrast, $M\Phi_{Tg}$ were found to exhibit an opposite landscape, encompassing an exaggerated pro-inflammatory and attenuated anti-inflammatory lipid profile that was associated with a macrophage M1 phenotype. These findings suggest that $iPLA_2\beta$ modulates the inflammatory lipid profile and raises the intriguing possibility that increased expression of $iPLA_2\beta$ in the β-cells can confer increased susceptibility of macrophages to activation.

EXPERIMENTAL PROCEDURES

Animals

Mouse breeders obtained from Dr. John Turk (Washington University School of Medicine, St. Louis, MO) were used to generate colonies of WT, *RIP.iPLA$_2\beta$.Tg* (selectively overexpressing $iPLA_2\beta$ in β-cells only), and global $iPLA_2\beta$-KO mice at the University of Alabama at Birmingham. Tg founders (TG1 line) were mated with WT C57BL/6J mice (Jackson Laboratory) to generate *RIP.iPLA$_2\beta$.Tg* (Tg) mice and WT mice, and male and female $iPLA_2\beta^{+/-}$ pairings were used to generate $iPLA_2\beta^{-/-}$ (KO) and $iPLA_2\beta^{+/+}$ (WT) mice, as previously described (43, 45). Prior to experimentation, the mice were genotyped, as described (44), utilizing primers described in **Table 1**. Animal experiments were conducted according to approved IACUC guidelines at the University of Alabama at Birmingham. As our earlier studies suggested differences between the WT generated by the two schemes, data from the KO and Tg genotypes were compared against their corresponding WT littermates.

Isolation and culture of peritoneal macrophages

Mice (7–8 weeks of age) were euthanized by CO_2 inhalation and cervical dislocation. Peritoneal macrophages were obtained by filling the peritoneal cavity with 5 ml of cold PBS containing 2% FBS, massaging gently, and withdrawing the cell-containing solution. Cells were pelleted at 300 *g* for 5 min and resuspended in growth medium [Eagle's minimum essential medium (Sigma-Aldrich; M0894), 2.0 mg/ml sodium bicarbonate (Fisher Scientific; BP328-500), 2 mM L-glutamine (Life Technologies; 25030-081), 100 U/ml penicillin-100 μg/ml streptomycin [Life Technologies; 15140-122), and 10% heat-inactivated FBS (Life Technologies; 16000044)] supplemented with 10% L929 cell-conditioned medium (source of M-CSF). Macrophages from a single collection were sufficient to seed six 60 mm nontreated culture dishes. Adherent macrophages appeared after 16 h of culture. All experiments were performed with expanded freshly isolated peritoneal macrophages under classical and alternate activation conditions, as described below. Macrophages isolated from WT, $iPLA_2\beta^{-/-}$ (KO), and *RIP.iPLA$_2\beta$.Tg* (Tg) mice are designated as $M\Phi_{WT}$, $M\Phi_{KO}$, and $M\Phi_{Tg}$, respectively.

TABLE 1. Genotyping primers

Name	Sequence (5′ to 3′)	Target	Product Size (bp)
WT-PLA2G6_F	AGCTTCAGGATCTCATGCCCATC	WT (KO) iPLA$_2$β	1,400
WT-PLA2G6_R	CTCCGCTTCTCGTCCCTCATGGA		
KO-Neo_F	TCGCCTTCTATCGCCTTCTTGAC	KO-iPLA$_2$β	400
KO-Ex_R	GGGGCCTCAGACTGGGAATC		
WT-PLA2G6_F	CCTCCGGAGAGCAGCGATTAAAAGTGTCAG	WT (Tg) iPLA$_2$β	450
WT-PLA2G6_R	TAGAGCTTTGCCACATCACAGGTCATTCAG		
Tg-PLA2G6_F	CTAGGCTCAGACATCATGCTGGACGAGGT	*RIP.iPLA$_2$β.Tg*	200
Tg-PLA2G6_R	AAGATCTCAGTGGTATTTGTGAGCCAGGG		

Macrophage activation

Macrophage activation was accomplished according to previously published methods (42). For classical activation, macrophages were treated with 15 ng/ml recombinant IFNγ (R&D Systems; 485-MI-100) for 8 h in growth medium followed by addition of 10 ng/ml ultrapure LPS (InvivoGen; tlrl-3pelps) and incubated for 16 h at 37°C. For alternative activation, macrophages were treated with 8 ng/ml recombinant IL-4 (R&D Systems; 404-ML-010) in growth medium for 16 h. Naïve macrophages, which received no activation stimuli, were maintained in growth medium with no additional treatment. In some experiments, the macrophages were pretreated for 1 h with either a secretory phospholipase A$_2$ (sPLA$_2$) (LY315920, 10 μM; Cayman Chemical) or cytosolic (c)PLA$_2$α (CAY 10502, 50 nM; Cayman Chemical) inhibitor prior to activation. The inhibitors were present during the entire activation period.

Macrophage mRNA target analyses

Macrophages cultured in 60 mm non-tissue culture-treated dishes were lysed in 1 ml of TRIzol (Life Technologies; 15596-026). Total RNA was prepared and purified using RNeasy mini kits (QIAGEN; 74104), and 1 μg RNA was converted to cDNA using the Superscript III first strand synthesis system (Life Technologies; 18080-051), according to manufacturer's instructions. The cDNA was diluted 10-fold and used as template in conventional or real-time quantitative PCR (qPCR). cDNA transcripts were amplified with primers (**Table 2**) designed using NCBI Primer-BLAST (https://www.ncbi.nlm.nih.gov/tools/primer-blast/). Real-time qPCR was carried out using SYBR Select Mastermix (Life Technologies; 4472908) according to the manufacturer's instructions. Relative gene expression levels were determined using the $2^{-\Delta\Delta Ct}$ method.

Eicosanoid preparation

Eicosanoids were extracted using a modified extraction process, as previously described (46, 47). Medium from cells (2 ml) was combined with an internal standard mixture comprised of 10% total volume methanol (200 μl) and glacial acetic acid (10 μl) before spiking with internal standard (20 μl) containing the following deuterated eicosanoids (2 pmol/μl, 40 pmol total) (all standards purchased from Cayman Chemicals): (d_4) 6-keto-PGF$_1$α, (d_4) PGF$_2$α, (d_4) PGE$_2$, (d_4) PGD$_2$, (d_8) 5-HETE, (d_8) 12-HETE, (d_8) 15-HETE, (d_6) 20-HETE, (d_{11}) 8,9-epoxyeicosatrienoic acid (EET), (d_8) 14,15-EET, (d_8) AA, (d_5) eicosapentaenoic acid, (d_5) DHA, (d_4) PGA$_2$, (d_4) LTB$_4$, (d_4) LTC$_4$, (d_4) LTD$_4$, (d_4) LTE$_4$, (d_5) 5(*S*),6(R)-lipoxin A$_4$, (d_{11}) 5-iPF2α-VI, (d_4) 8-iso PGF$_2$α, (d_{11}) (±)14,15-dihydroxyeicosatrienoic acid (DHET), (d_{11}) (±)8,9-DHET, (d_{11}) (±)11,12-DHET, (d_4) PGE$_1$, (d_4) thromboxane B$_2$ (TXB$_2$), (d_6) dihomo-γ linoleic acid, (d_5) resolvin D2, (d_5) resolvin D1, (d_5) maresin2, and (d_5) resolvin D3. Samples and vial rinses (5% methanol; 2 ml) were applied to Strata-X SPE columns (Phenomenex) previously washed with methanol (2 ml) and then dH$_2$O (2 ml). Eicosanoids eluted with isopropanol (2 ml), were dried in vacuo and reconstituted in ethanol:dH$_2$O (50:50;100 μl) prior to ultra-performance (UP)LC ESI-MS/MS analysis.

Analysis of eicosanoids by UPLC ESI-MS/MS

Eicosanoids were separated using a Shimadzu Nexera X2 LC-30AD coupled to a SIL-30AC auto injector, coupled to a DGU-20A5R degassing unit in the following way [as previously described by us (47)]. A 14 min reversed phase LC method utilizing an Acentis Express C18 column (150 × 2.1 mm, 2.7 μm) was used to separate the eicosanoids at a 0.5 ml/min flow rate at 40°C as we previously described (47). The column was equilibrated with 100% solvent A [acetonitrile:water:formic acid (20:80:0.02, v/v/v)] for 5 min and then 10 μl of sample were injected. Solvent A (100%) was used for the first 2 min of elution. Solvent B [acetonitrile:isopropanol:formic acid (20:80:0.02, v/v/v)] was increased in a linear gradient to 25% solvent B at 3 min, to 30% at 6 min, to 55% at 6.1 min, to 70% at 10 min, and to 100% at 10.10 min. Solvent B (100%) was held constant until 13.0 min, where it was decreased to 0% solvent B and 100% solvent A from 13.0 min to 13.1 min. From 13.1 min to 14.0 min, solvent A was held constant at 100%. All solvents were purchased from Fischer Scientific.

TABLE 2. Real-time qPCR primers

Name	Sequence (5′ to 3′)	T_m (salt)	Target
msMRC1.F	GTCAGAACAGACTGCGTGGA	60.0	*Mrc1*
msMRC1.R	AGGGATCGCCTGTTTTCCAG	60.0	
msARG2.F	GCAAATTCCTTGCGTCCTGA	60.0	*Arg2*
msARG2.R	AGGCCCACTGAACGAGGATA	60.0	
msPtgs2.F3	TGAGTGGGGTGATGAGCAAC	60.0	*PTGS2*
msPtgs2.R3	TTCAGAGGCAATGCGGTTCT	60.0	
ALOX12.F	GGCTATCCAGATTCAGCCCC	60.0	*ALOX-12*
ALOX12.R	CCGGCTTCGCGTGTTAATTT	57.1	
miPLA$_2$.F	TATGCGTGGTGTGATCTTCCG	57.1	*iPLA$_2$β*
miPLA$_2$.R	CATGGAGCTCAGGATGAACGC	60.0	
msPLA$_2$ GV.F (101)	AGCCTCGATCATGGCCTTT	56.8	*GV sPLA$_2$*
msPLA$_2$ GV.R (101)	GCCGAATCATTTCCCCAAA	56.8	
mcPLA$_2$.F	CCCTGAGTAGTTTGAAGGAAAAGG	55.4	*cPLA$_2$*
mcPLA$_2$.R	ACACGTGAAGAGAGGCAAAGG	55.4	

Eicosanoids were analyzed via MS using an AB Sciex Triple Quad 5500 mass spectrometer, as previously described by us (47). Q1 and Q3 were set to detect distinctive precursor and product ion pairs. Ions were fragmented in Q2 using N_2 gas for collisionally induced dissociation. Analysis used multiple-reaction monitoring in negative-ion mode. Eicosanoids were monitored using precursor → product MRM pairs. The mass spectrometer parameters used were: curtain gas, 20 psi; CAD, medium; ion spray voltage, −4,500 V; temperature, 300°C; gas 1, 40 psi; gas 2, 60 psi (declustering potential, entrance potential, collision energy, and cell exit potential varied per transition). MRM transitions with corresponding declustering potentials, collision energies, entrance potentials, and collision cell exit potentials are shown in supplemental Table S1.

Selectivity of transgene function

As described (43), to generate Tg mice with selective overexpression of iPLA$_2$β in β-cells only, rat iPLA$_2$β cDNA was inserted downstream of the rat insulin promoter (RIP) at a site within the rabbit globin gene sequence. As such, transcription of the sequence encoding iPLA$_2$β is under control of RIP, and transgenic overexpression of iPLA$_2$β is expected only in cells that express insulin, i.e., pancreatic islet β-cells, but not in other cells (i.e., macrophages). To verify that induction of the transgene was specific to β-cells, PCR analyses were performed using islet and macrophage cDNA as a template with two pairs of primers. One pair amplified the sequence in the internal control fatty acid-binding protein, intestinal (*Fabpi*) gene, and the primer sequences were (*Fabpi* 5′) cctccggagagcagcgattaaaagtgtcag and (*Fabpi* 3′) tagagctttgccacatcacaggtcattcag (expected product size, 450 bp). The other primer pair amplified a sequence that spanned the junction of iPLA$_2$β and globin cDNA in the TG construct. The primer sequences were (TG 5′) ctaggctcagacatcatgctggacgaggt and (TG 3′) aagatctcagtggtatttgtgagccaggg (expected product size, 200 bp). Subsequently, the islets and macrophages were processed for insulin content and iPLA$_2$β immunoblotting (1° antibodies: iPLA$_2$β, E-8, sc-166616; tubulin, TU-02, sc-8035) analyses, as described (48, 49).

Statistical analysis

Lipidomics samples were analyzed via a multivariate approach using SPSS. In experiments with more than two conditions, samples were analyzed by ANOVA on the R platform with a Tukey's post hoc test. In experiments using two conditions, samples were analyzed using a Student's *t*-test. Presented data are mean ± SEM and, where appropriate, as fold-change relative to control (vehicle). Values of $P < 0.05$ were considered significant.

RESULTS

iPLA$_2$β$^{-/-}$ model verification

As previously reported (43, 45), DNA was generated from tail clips and progeny were genotyped by PCR analyses. The primers used for the WT or for the disrupted iPLA$_2$β$^{-/-}$ (KO) sequence were expected to yield product sizes of 1,400 or 400 bp, respectively. Consistently, only a 1,400 bp product in WT (lanes 1 and 2) and a 400 bp product in KO (lanes 3 and 4) were evident (**Fig. 1**). The iPLA$_2$β$^{-/-}$ group is referred to as KO and macrophages isolated from these mice as MΦ$_{KO}$, and macrophages from WT, MΦ$_{WT}$.

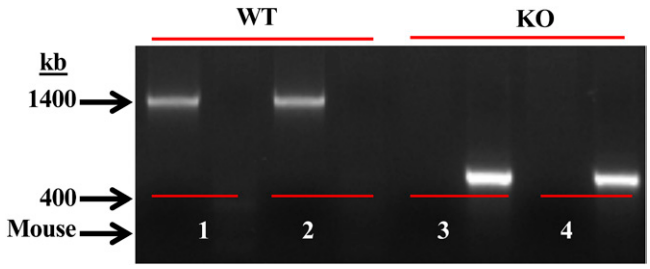

Fig. 1. Genotyping and verification of the iPLA$_2$β$^{-/-}$ model. DNA was generated from tail clips and progeny were genotyped by PCR analyses. Reactions were performed in the presence of primers for the WT sequence (sets 1 and 2) or for the disrupted KO sequence (sets 3 and 4) for each mouse. The expected bands for WT (1,400 bp) and KO (400 bp) in two mice each are presented.

Comparison of basal lipid species in WT and KO

The MS protocol identified several lipid species (**Table 3**), including pro-inflammatory and anti-inflammatory PGs, LTs, HETEs, DHETs, EETs, and specialized pro-resolving lipid mediators (SPMs). Analyses of lipid production under basal conditions revealed no significant differences in the abundances of detected lipids between WT and KO (supplemental Table S2). These findings suggest an overall similar profile in MΦ$_{WT}$ and MΦ$_{KO}$ production of lipids.

Comparison of pro-inflammatory lipid production from activated MΦ$_{WT}$ and MΦ$_{KO}$

AA, subsequent to its release from membrane glycerophospholipids, can be metabolized by COXs and LOs to generate oxidized bioactive products, designated eicosanoids. Some of these lipids are considered to be pro-inflammatory. They include several PGs, LTs, and HETEs (Table 3). Further, epoxidation of AA by cytochrome P450 epoxygenases leads to the generation of EETs, which are then hydrolyzed by soluble epoxide hydrolases to pro-inflammatory DHETs. Comparison of macrophage pro-inflammatory lipid production in response to classical activation revealed an increase in pro-inflammatory PGs generated by both MΦ$_{WT}$ and MΦ$_{KO}$ in response to IFNγ + LPS (**Fig. 2A**). However, the increase in PGE$_2$ in the KO group was of lower magnitude relative to the WT group. Overall, a nearly 40% lower production of pro-inflammatory PGs (pool of PGs presented in Fig. 2A) by MΦ$_{KO}$ relative to MΦ$_{WT}$ was evident (Fig. 2B). However, production of other pro-inflammatory lipid species, including LTs (**Fig. 3**), HETEs (supplemental Fig. S1A), or DHETs (±14,15 and ±11,12; supplemental Fig. S2A), by MΦ$_{KO}$ was similar to MΦ$_{WT}$, and the production of (±)8,9-DHET by MΦ$_{KO}$ was higher relative to MΦ$_{WT}$. These observations suggest that iPLA$_2$β promotes production of select pro-inflammatory PGs in macrophages.

Comparison of anti-inflammatory lipid production from activated WT and MΦ$_{KO}$

In addition to generation of pro-inflammatory lipids, metabolism of AA can generate anti-inflammatory lipids (Table 3), such as EETs, which have been reported to manifest anti-inflammatory properties (50). Further, dihomo-γ-linolenic acid (DHGLA) can be converted to PGE$_1$, and

TABLE 3. Macrophage lipids identified by UPLC ESI-MS/MS analyses

	Lipid Species
Pro-inflammatory	
PGs	6-keto $PGF_1\alpha$, TXB_2, $PGF_2\alpha$, 8-iso $PGF_2\alpha$, 5-$iPF_2\alpha$-VI, PGE_2, PGD_2, PGA_2, 15-deoxy-Δ12,14-PGJ_2
LTs	LTB_4, LTC_4, LTD_4, LTE_4
Dihydoxyeicosatrienoic acids	(±)11,12-DHET, (±)14,15-DHET, (±)8,9-DHET
Hydoxyeicosatrienoic acids	20-HETE, 15-HETE, 12-HETE, 5-HETE
Anti-inflammatory	
PGs	PGE_1
SPMs	Resolvin D2, resolvin D1, lipoxin A_4
EETs	(±)11,12-EET, (±)14,15-EET, (±)8,9-EET

SPMs are generated via metabolism of AA (lipoxin A_4) or DHA (resolvins D_1 and D_2). With classical activation, anti-inflammatory PGs increased similarly in the WT and KO (**Fig. 4A**). In contrast, production of resolvin D_2 by $M\Phi_{KO}$ was significantly higher (Fig. 4B) relative to $M\Phi_{WT}$; whereas, production of EETs was similar between WT and KO (supplemental Fig. S2B). Further, alternative activation did not promote differential changes in the production of SPMs (data not shown). These observations suggest that $iPLA_2\beta$ can modulate macrophage production of select SPMs.

$iPLA_2\beta^{-/-}$ (KO) macrophage phenotype

As expected, real-time qPCR analyses (**Fig. 5A**) confirmed a relative absence of $iPLA_2\beta$ mRNA in $M\Phi_{KO}$ under both basal and activated conditions. $iPLA_2\beta$ mRNA in $M\Phi_{WT}$ was modestly, but not significantly, affected by classical activation (approximately 25% increased) and alternative activation (approximately 25% decreased) relative to basal expression. We previously demonstrated that classical activation of macrophages promotes an M1 inflammatory phenotype, whereas alternative activation favors an M2 anti-inflammatory phenotype (42). To confirm that macrophages used in the present lipid analyses exhibited the expected phenotype, they were stimulated with IFNγ + LPS or IL-4 and the macrophages were assessed for expression of markers for M1 [arginase 2 (*Arg2*)] and M2 [mannose receptor C type 1 (*MRC1*)], respectively, by real-time qPCR. Activation induced the corresponding markers in $M\Phi_{WT}$ and $M\Phi_{KO}$; however, relative expression of *Arg2* was reduced (Fig. 5B) and *MRC1* increased (Fig. 5C) in $M\Phi_{KO}$ in comparison with $M\Phi_{WT}$. These findings are consistent with the reduced pro-inflammatory lipid profile in the KO. However, induction of *Arg2* and *MRC1* in

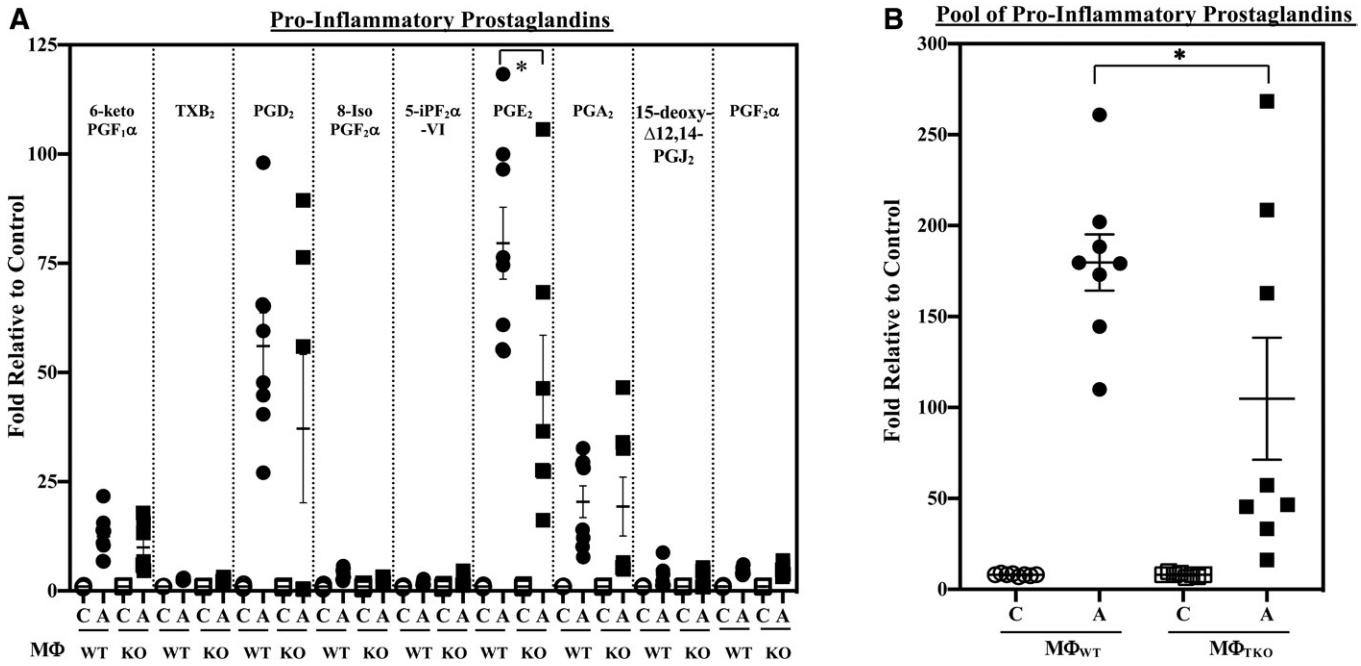

Fig. 2. Pro-inflammatory PG production by $M\Phi_{WT}$ and $M\Phi_{KO}$. Peritoneal macrophages isolated from 8-week-old WT and KO mice were treated with vehicle [control (C)] or IFNγ + LPS and the media collected for lipidomics analyses. The data represent activated (A) fold-changes in lipids relative to C. A: Individual PGs. Control (pmol lipid/$1e^{+06}$) $M\Phi_{WT}$ and $M\Phi_{KO}$: 6-keto $PGF_1\alpha$, 2.512 ± 0.302 and 3.818 ± 0.564; TXB_2, 4.563 ± 0.585 and 4.491 ± 0.538; PGD_2, 0.568 ± 0.083 and 0.881 ± 0.128; 8-Iso $PGF_2\alpha$, 0.056 ± 0.008 and 0.059 ± 0.013; 5-$IPF_2\alpha$-VI, 0.263 ± 0.033 and 0.301 ± 0.068; PGE_2, 1.213 ± 0.313 and 1.690 ± 0.349; PGA_2, 0.472 ± 0.035 and 0.525 ± 0.050; 15-deoxyΔ12,14-PGJ_2, 0.253 ± 0.087 and 0.240 ± 0.072; $PGF_2\alpha$, 0.646 ± 0.055 and 0.591 ± 0.032. B: PG pool. Control (pmol lipid/$1e^{+06}$) $M\Phi_{WT}$ and $M\Phi_{KO}$: 3.804 ± 0.253 and 4.564 ± 0.443. Data are mean ± SEM determined from seven to nine independent experiments. *$M\Phi_{KO}$ significantly different from $M\Phi_{WT}$, $P < 0.05$).

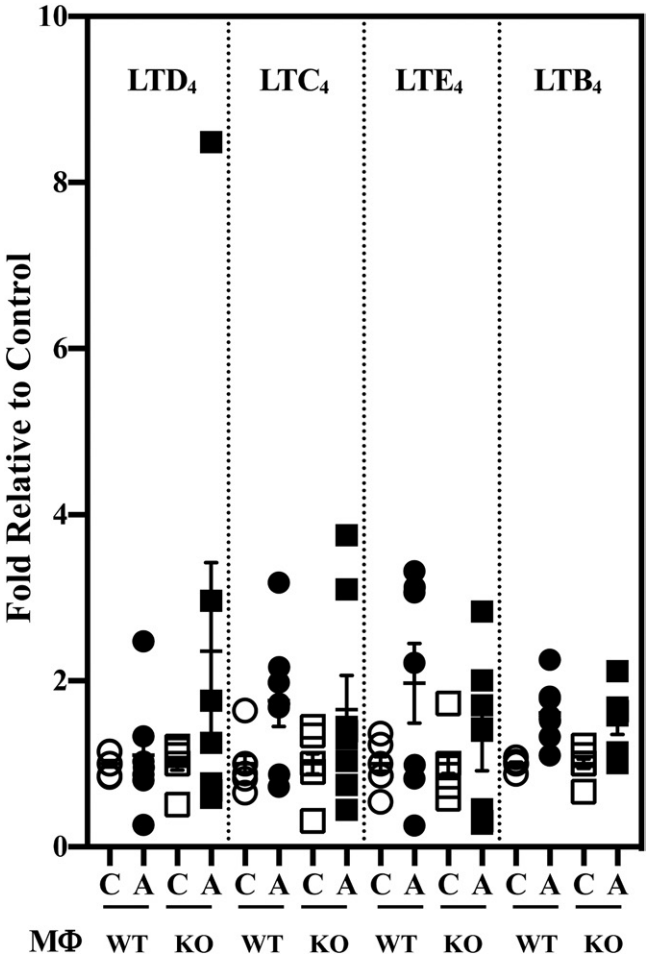

Fig. 3. LT production by $M\Phi_{WT}$ and $M\Phi_{KO}$. Peritoneal macrophages isolated from 8-week-old WT and KO mice were treated with vehicle [control (C)] or IFNγ + LPS and the media collected for lipidomics analyses. The data represent activated (A) fold-changes in lipids relative to C. Control (pmol lipid/$1e^{+06}$) $M\Phi_{WT}$ and $M\Phi_{KO}$: LTD4, 0.072 ± 0.028 and 0.072 ± 0.027; LTC_4, 0.022 ± 0.005 and 0.019 ± 0.005; LTE_4, 0.101 ± 0.016 and 0.158 ± 0.038; LTB_4, 0.429 ± 0.074 and 0.573 ± 0.118. Data are mean ± SEM determined from seven to nine independent experiments.

$M\Phi_{WT}$ and $M\Phi_{KO}$ by alternative and classical activation, respectively, was similar (supplemental Fig. S3A, B).

RIP.iPLA$_2$β.Tg (Tg) model verification

In view of the observed effects on macrophage lipid production associated with $iPLA_2\beta$-deficiency and literature evidence for intercellular communication between inflamed sites and immune cells, we explored the possibility that signals generated by β-cells could manifest effects in macrophages. To address this, we compared lipid production from $M\Phi_{Tg}$ and $M\Phi_{WT}$ littermates. We previously demonstrated that the Tg mice overexpress $iPLA_2\beta$ selectively in β-cells (44). To assess the genotype of the *RIP.iPLA$_2$β.Tg* (Tg), PCR analyses were performed in the presence of two sets of primers expected to yield product sizes of 450 and 200 bp for the WT (**Fig. 6**, lanes 1–3) and the *RIP.iPLA$_2$β.Tg* (Fig. 6, lanes 4–6), respectively. Such analyses (Fig. 6) revealed only a 450 bp band in the WT and a 200 bp in the Tg. The *RIP.iPLA$_2$β.Tg* group is referred to as Tg and macrophages isolated from these mice as $M\Phi_{Tg}$.

Comparison of basal lipid species in WT and Tg

Because the KO and Tg mice were derived through different breeding schemes, the Tg mice were compared with their own littermate WT mice. Lipidomics analyses of basal production of lipids revealed no significant differences in the abundances of lipids between $M\Phi_{WT}$ and $M\Phi_{Tg}$ (supplemental Table S3). These findings suggest that similar to $M\Phi_{KO}$, inherent production of lipids by $M\Phi_{Tg}$ is unaffected.

Comparison of pro-inflammatory lipid production from activated WT and $M\Phi_{Tg}$

Classical activation of the macrophages promoted higher production of select pro-inflammatory PG lipids (6-keto$PGF_1\alpha$ and PGE_2) by $M\Phi_{Tg}$ relative to $M\Phi_{WT}$ (**Fig. 7A**). Though PGD_2 production by $M\Phi_{Tg}$ was decreased, there was an overall 2-fold higher production of pro-inflammatory PGs (pool of PGs presented in Fig. 7A) by $M\Phi_{Tg}$ relative to $M\Phi_{WT}$ (Fig. 7B). Further, while LTD_4, LTC_4, and LTE_4 production was similar in $M\Phi_{WT}$ and $M\Phi_{Tg}$ (**Fig. 8**), LTB_4 was significantly elevated in $M\Phi_{Tg}$ relative to $M\Phi_{WT}$. However, production of HETEs (supplemental Fig. S1B) or DHETs (supplemental Fig. S4A) was not significantly different between $M\Phi_{WT}$ and $M\Phi_{Tg}$. These observations suggest that $M\Phi_{Tg}$ are primed to respond to classical activation.

Comparison of anti-inflammatory lipid production from activated WT and $M\Phi_{Tg}$

Classical activation increased PGE_1 production by $M\Phi_{Tg}$ relative to $M\Phi_{WT}$ (**Fig. 9A**), but the production of SPMs by $M\Phi_{WT}$ and $M\Phi_{Tg}$ was similar (data not shown). Alternative activation promoted a 3-fold increase in resolvin D2 production by $M\Phi_{WT}$; however, its production by $M\Phi_{Tg}$ was unchanged from basal production (Fig. 9B). EETs were not significantly different between $M\Phi_{WT}$ and $M\Phi_{Tg}$ (supplemental Fig. S4B). These observations suggest that $M\Phi_{Tg}$ are predisposed to differential generation of PGE_1, derived from DHGLA, and select SPMs.

Impact of $sPLA_2$ and $cPLA_2\alpha$ on macrophage lipid profiles

Noting that other PLA_2s may also contribute to the altered lipid profile, we sought to determine whether $sPLA_2$s or $cPLA_2\alpha$s contribute to the observed changes in eicosanoid production by $M\Phi_{Tg}$. The C57BL/J6 macrophages are reported to express GV and GX $sPLA_2$ (51, 52) and $cPLA_2\alpha$ (16), but not GIIA $sPLA_2$ (51, 53–56). mRNA analyses revealed that $sPLA_2$ mRNA in $M\Phi_{Tg}$ was not altered under basal or activated conditions, whereas $cPLA_2$ mRNA was higher under basal but similar under activated conditions relative to $M\Phi_{WT}$ (**Fig. 10**). We next determine whether the lipid profiles of $M\Phi_{WT}$ and $M\Phi_{Tg}$ were modulated by inhibitors of $sPLA_2$ [LY315920 (57), which inhibits several $sPLA_2$s including GIIA, GV, and GX] or $cPLA_2\alpha$ [CAY 10502 (58)]. Lipidomics analyses revealed that neither basal (**Table 4**) nor activated (**Table 5**) production of lipids by $M\Phi_{WT}$ and $M\Phi_{Tg}$ was affected by LY315920

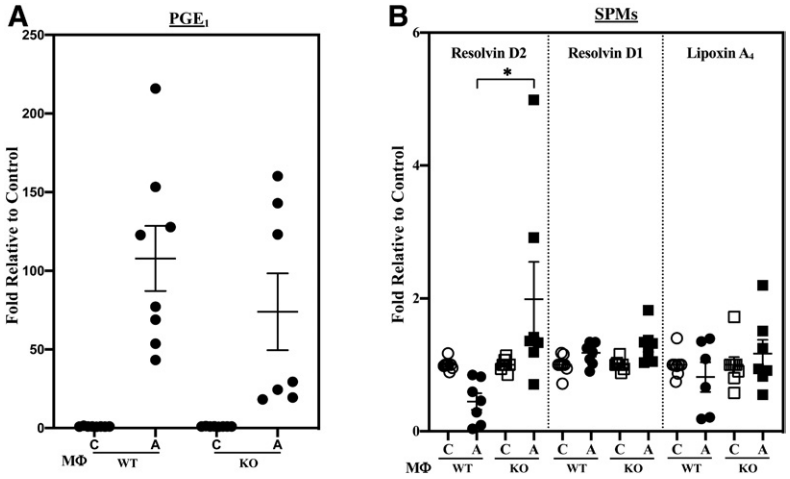

Fig. 4. Production of anti-inflammatory PGE_1 and SPMs by $M\Phi_{WT}$ and $M\Phi_{KO}$. Peritoneal macrophages isolated from 8-week-old WT and KO mice were treated with vehicle [control (C)] or IFNγ + LPS and the media collected for lipidomics analyses. The data represent activated (A) fold-changes in lipids relative to C. A: PGE_1 ± IFNγ + LPS. Control (pmol lipid/$1e^{+06}$) $M\Phi_{WT}$ and $M\Phi_{KO}$: 0.162 ± 0.020 and 0.240 ± 0.021. B: SPMs. Control (pmol lipid/$1e^{+06}$) $M\Phi_{WT}$ and $M\Phi_{KO}$: resolvin D2, 0.110 ± 0.029 and 0.100 ± 0.032; resolvin D1, 0.100 ± 0.013 and 0.115 ± 0.019; lipoxin A_4, 0.235 ± 0.065 and 0.288 ± 0.109. Data are mean ± SEM determined from seven to nine independent experiments. *$M\Phi_{KO}$ significantly different from $M\Phi_{WT}$, $P < 0.05$.

or CAY 10502. Comparisons between $M\Phi_{WT}$ and $M\Phi_{Tg}$ exposed to LY315920 revealed a higher basal production of several pro-inflammatory PGs and LTE_4 by $M\Phi_{Tg}$ relative to $M\Phi_{WT}$ (Table 4). In contrast, basal production of lipids by $M\Phi_{WT}$ and $M\Phi_{Tg}$ exposed to CAY 10502 was unaffected. Classical activation resulted in increases in lipid production by both $M\Phi_{WT}$ and $M\Phi_{Tg}$ (Table 5), with production by $M\Phi_{Tg}$ significantly higher relative to $M\Phi_{WT}$. Such increases were maintained in the presence of LY315920 or CAY 10502. These findings suggest that GV and GX $sPLA_2$s and $cPLA_2\alpha$ are not likely contributors to the inflammatory lipid profile in activated $M\Phi_{Tg}$.

Phenotype comparison of $M\Phi_{WT}$ and $M\Phi_{Tg}$

In view of the observations that $M\Phi_{Tg}$ exhibit a higher inflammatory state, we assessed macrophage phenotype with activation. We found that classical activation of $M\Phi_{Tg}$ promoted a greater induction of the M1 marker *Arg2* (**Fig. 11A**), while the M2 marker *MRC1* was reduced with alternative activation (Fig. 11B) relative to $M\Phi_{WT}$. Whereas, induction of *Arg2* in $M\Phi_{WT}$ and $M\Phi_{Tg}$ by alternative activation was not different, induction of *MRC1* by classical activation was reduced in the $M\Phi_{Tg}$ (supplemental Fig. S3C, D). These findings are consistent with a heightened pro-inflammatory and reduced anti-inflammatory lipid profile in $M\Phi_{Tg}$. No differences were observed in the expression of *ALOX-12* or *PTGS2* mRNA, which encode 12-LO and COX2, respectively, in $M\Phi_{WT}$ and $M\Phi_{Tg}$ under basal (**Fig. 12A**) or activated (Fig. 12B, C) conditions. Under both basal and activated conditions, $iPLA_2\beta$ mRNA was modestly and similarly increased in $M\Phi_{Tg}$ (Fig. 12D) relative to $M\Phi_{WT}$. To determine whether the transgene is induced in $M\Phi_{Tg}$, PCR, insulin content, and $iPLA_2\beta$ immunoblotting analyses were performed in islets and macrophages isolated from WT and Tg mice. As expected, transgene expression was evident in both islets and macrophages from Tg mice but not from WT mice (**Fig. 13A**). However, as islet β-cells but not macrophages produce insulin (Fig. 13B), overexpression of $iPLA_2\beta$ protein was only detected in the islets and not in the $M\Phi_{Tg}$ relative to $M\Phi_{WT}$ (Fig. 13C). These findings suggest that signals generated by $iPLA_2\beta$-overexpressing β-cells, upon appropriate stimulation, prime macrophages to adopt an M1 phenotype, independent of transgene leakage.

DISCUSSION

Inflammatory processes play critical roles in promoting autoimmune-mediated β-cell death leading to T1D; however, the underlying mechanisms promoting inflammation are not well understood. Eicosanoids are recognized contributors to inflammatory responses (4, 59, 60) and these

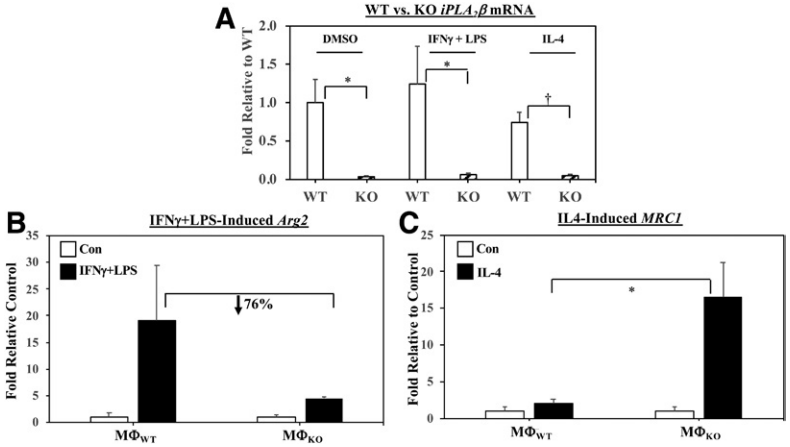

Fig. 5. Induction of M1 (*Arg2*) and M2 (*MRC1*) markers and $iPLA_2\beta$ in $M\Phi_{WT}$ and $M\Phi_{KO}$. Peritoneal macrophages isolated from 8-week-old WT and KO mice were treated with vehicle [control (Con)], IFNγ + LPS, or IL-4. The cells were harvested and processed for real-time qPCR analyses. A: *$iPLA_2\beta$* . B: *Arg2* ($M\Phi_{WT}$ and $M\Phi_{KO}$ *Arg2* $2^{-\Delta\Delta CT}$, 0.095 ± 0.074 and 1.506 ± 0.558.) C: *MRC1* ($M\Phi_{WT}$ and $M\Phi_{KO}$ *MRC1* $2^{-\Delta\Delta CT}$, 4.273 ± 2.357 and 16.053 ± 10.294). Data are mean ± SEM of fold-change relative to Con determined from four independent experiments. *$M\Phi_{KO}$ significantly different than $M\Phi_{WT}$ group, $P < 0.05$; †$M\Phi_{KO}$ significantly different than $M\Phi_{WT}$ group, $P < 0.005$.

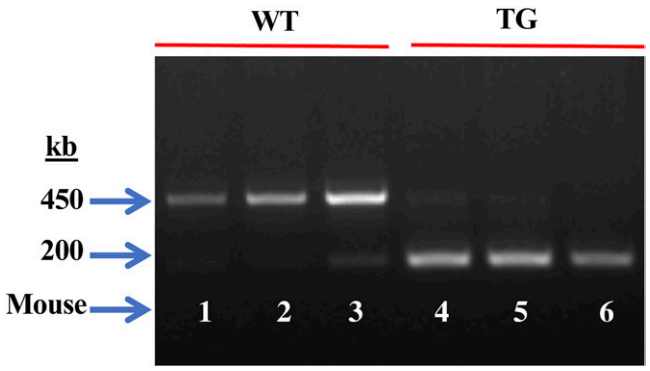

Fig. 6. Genotyping and verification of the *RIP.iPLA$_2$β.Tg* model. DNA was generated from tail clips and progeny were genotyped by PCR analyses. Reactions were performed in the presence of two sets of primers and the expected bands for WT (lanes 1–3, 450 bp) and Tg (lanes 4–6, 200 bp) in three mice each are presented.

bioactive lipids are generated via metabolism of AA, following its release from membrane glycerophospholipids by a PLA$_2$-mediated mechanism. We reported that activation of iPLA$_2$β participates in β-cell death due to ER stress and pro-inflammatory cytokines (44, 61, 62), which are key contributors to β-cell demise leading to T1D. We also observed that activation of iPLA$_2$β promotes an M1 inflammatory macrophage phenotype, whereas iPLA$_2$β deficiency favors an M2 anti-inflammatory phenotype (42). Consistent with these reports, selective inhibition of iPLA$_2$β was found to markedly reduce insulitis, CD4$^+$ T-cell and B-cell responses, and diabetes incidence in the nonobese diabetic (NOD) mouse model, a spontaneous autoimmune diabetes-prone mouse model of T1D (20). Collectively, these findings suggested a prominent role for iDLs in promoting inflammatory responses.

Eicosanoids generated via metabolism of AA by COX and 12-LO are recognized to play significant roles in a variety of inflammatory diseases, including diabetes, cancer, atherosclerosis, osteoporosis, and EAE (3, 5, 41, 60, 63–66). The most potent of the inflammatory lipids include PGs, LTs, HETEs, and DHETs. Roles ascribed to them include promoting CD4 Th1/Th17 differentiation (67), inhibition of Tr1 differentiation (68), inducing NF-κB (69), inhibiting Treg cell differentiation (70), modulating local activation of T-cells (71), inducing NO (72), participating in oxidative stress pathways (73), increasing expression of cytokine genes and monocyte chemoattractant protein 1 (74, 75), and reducing inflammation-resolving processes (76–79). In contrast, other PGs (i.e., PGE$_1$), SPMs, and EETs are involved in resolving inflammation (50, 80–82).

Our collection of earlier findings suggests that iDLs are key contributors to inflammation, β-cell death, and subsequent development of T1D. While eicosanoids have been linked with inflammation development (46, 83), to date, very little is known about the eicosanoid profile of activated macrophages and whether iDLs contribute to an inflammatory state. Therefore, in view of our findings of a link between iPLA$_2$β and macrophage polarization and responses, we utilized a targeted lipidomics approach with

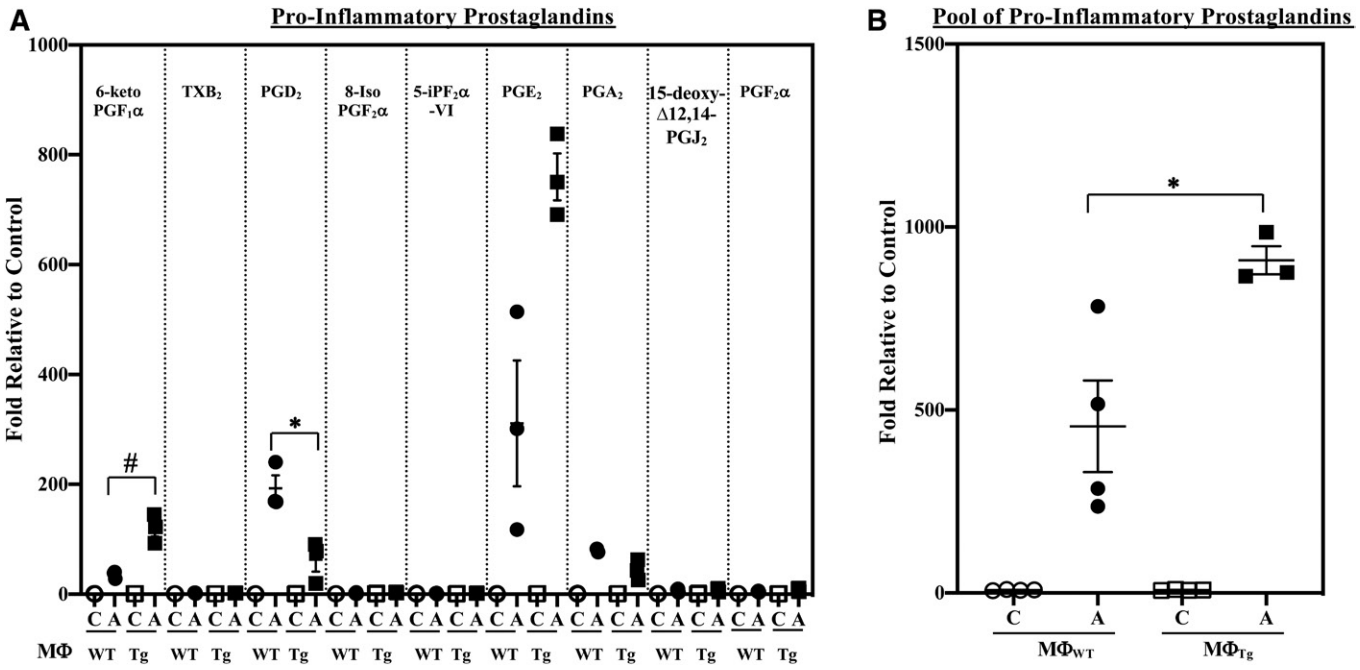

Fig. 7. Pro-inflammatory PG production by MΦ$_{WT}$ and MΦ$_{Tg}$. Peritoneal macrophages isolated from 8-week-old WT and Tg mice were treated with vehicle [control (C)] or IFNγ + LPS and the media collected for lipidomics analyses. The data represent activated (A) fold-changes in lipids relative to C. Data are mean ± SEM determined from three to four independent experiments. A: Individual PGs. Control (pmol lipid/1e^{+06}) MΦ$_{WT}$ and MΦ$_{Tg}$: 6-keto PGF$_1$α, 0.502 ± 0.179 and 0.462 ± 0.069; TXB$_2$, 3.725 ± 0.206 and 4.139 ± 0.152; PGD$_2$, 0.036 ± 0.006 and 0.039 ± 0.008; 8-Iso PGF$_2$α, 0.131 ± 0.006 and 0.103 ± 0.039; 5-IPF$_2$α-VI, 0.200 ± 0.082 and 0.162 ± 0.030; PGE$_2$, 0.147 ± 0.044 and 0.083 ± 0.008; PGA$_2$, 0.177 ± 0.068 and 0.139 ± 0.018; 15-deoxyΔ12,14-PGJ$_2$, 0.028 ± 0.006 and 0.037 ± 0.012; PGF$_2$α, 4.587 ± 0.784 and 3.856 ± 0.448. $^{\#}$MΦ$_{Tg}$ significantly different from MΦ$_{WT}$, $P < 0.01$; *MΦ$_{Tg}$ significantly different from MΦ$_{WT}$, $P < 0.05$. B: PG pool. Control (pmol lipid/1e^{+06}) MΦ$_{WT}$ and MΦ$_{Tg}$: 9.533 ± 0.153 and 9.019 ± 0.087. *MΦ$_{Tg}$ significantly different from MΦ$_{WT}$, $P < 0.05$.

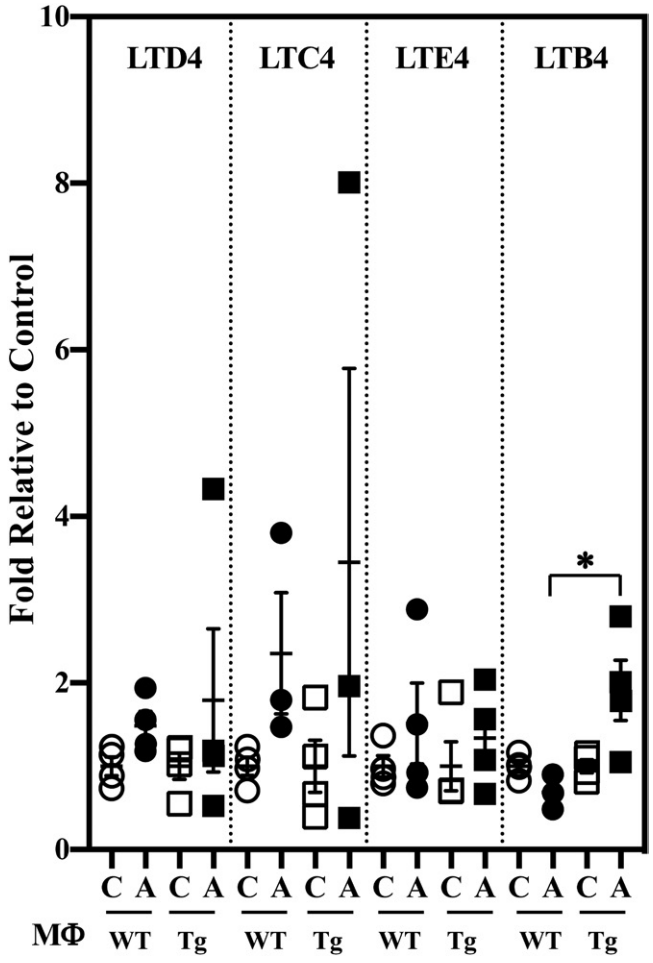

Fig. 8. LT production by $M\Phi_{WT}$ and $M\Phi_{Tg}$. Peritoneal macrophages isolated from 8-week-old WT and Tg mice were treated with vehicle [control (C)] or IFNγ + LPS and the media collected for lipidomics analyses. The data represent activated (A) fold-changes in lipids relative to C. Control (pmol lipid/$1e^{+06}$) $M\Phi_{WT}$ and $M\Phi_{Tg}$: LTD_4, 0.0020 ± 0.0001 and 0.0060 ± 0.0001; LTC_4, 0.011 ± 0.002 and 0.016 ± 0.005; LTE_4, 0.009 ± 0.002 and 0.009 ± 0.002; LTB_4, 0.229 ± 0.015 and 0.188 ± 0.015. Data are mean ± SEM determined from four independent experiments. *$M\Phi_{Tg}$ significantly different from $M\Phi_{WT}$, $P < 0.05$.

commercially available eicosanoid standards and WT, *iPLA$_2$β$^{-/-}$* (KO), and *RIP.iPLA$_2$β.Tg* (Tg) mouse models to identify iDLs generated by activated macrophages. Our studies revealed two salient and previously undescribed features: *1*) the predominant anti-inflammatory M2 phenotype due to iPLA$_2$β-deficiency is associated with reduced generation of select pro-inflammatory eicosanoids and increased production of the SPM, resolvin D2; and *2*) greater production of select pro-inflammatory eicosanoids and reduced resolvin D2 from $M\Phi_{Tg}$ is associated with macrophage polarization toward the inflammatory M1 phenotype. These findings, for the first time, reveal an association between selective changes in eicosanoids and SPMs with macrophage polarization and, further, that the relevant lipid species are modulated by iPLA$_2$β activity. Most importantly, our findings unveil the possibility that events triggered in β-cells can modulate macrophage responses. This is supported by observations in the *RIP.iPLA$_2$β.Tg* model with a select overexpression of iPLA$_2$β in β-cells; yet, macrophages from these mice exhibit an opposite spectrum relative to $M\Phi_{KO}$. To our knowledge, this is the first demonstration of intercellular signaling, in particular iPLA$_2$β-derived intercellular signaling, originating from β-cells affecting macrophage function.

iPLA$_2$β deficiency, verified by genotype and real-time qPCR analyses, was associated with a significant reduction in the pool of pro-inflammatory PGs with a selective decrease in the abundance of PGE_2. Other recognized inflammatory lipids, including LTs and DHETs, were not significantly affected by iPLA$_2$β deficiency. While there were no significant differences in the induction of anti-inflammatory PGs by $M\Phi_{WT}$ and $M\Phi_{KO}$, production of resolvin D2 by $M\Phi_{KO}$ in response to classical activation was significantly higher relative to $M\Phi_{WT}$. These lipid changes are associated with decreased *Arg2* (M1 marker) and increased *MRC1* (M2 marker) in $M\Phi_{KO}$. Resolvin D_2 arises from the metabolism of DHA, and lipids containing DHA are substrates for iPLA$_2$β (84). However, sPLA$_2$s exhibit greater activity toward lipids containing DHA than does iPLA$_2$β (84), and the group V and IIa sPLA$_2$s are activated during inflammation (85, 86). Consistent with this premise, it has been suggested that at the onset of inflammation, iPLA$_2$β activity predominates and leads to increased production of inflammatory lipids (2). However, a subsequent resolution phase is unmasked during which groups IIA and V sPLA$_2$s are activated. Taken together with our present findings, it is likely that iPLA$_2$β deficiency is permissive for sPLA$_2$ activation to affect resolution through generation of resolvin D_2. This latter phase appears to occur in the absence of increased expression of sPLA$_2$s, at least at the time point studied. Acknowledging that in vitro systems are artificial and limited, we speculate that the in vivo inflammatory landscape gives rise to a more dramatic lipid profile.

Intriguingly, we found that the production of pro-inflammatory lipids by $M\Phi_{Tg}$ was increased. These included 6-keto $PGF_1\alpha$, PGE_2, and LTB_4. Concurrently, there was increased production of anti-inflammatory PGE_1 but decreased production of PGD_2, suggesting differential regulation of pathways leading to generation of these PGs during inflammation. The increase in PGE_1 most likely reflects an attempt at resolution (87). Interestingly, in contrast to $M\Phi_{KO}$, resolvin D2 production by $M\Phi_{Tg}$ was not altered with classical activation, but was significantly reduced under alternative activation. This suggests a decrease in the metabolism of DHA, which has been reported to increase susceptibility to inflammation (88, 89). In our earlier study, we observed that the polarization toward M2 macrophage phenotype with iPLA$_2$β deficiency was not a direct effect on iDL production, but was most likely due to the overall decrease in an inflammatory state, which is permissive for the evolution of anti-inflammatory processes (42). The differential production of resolvin D2 by $M\Phi_{KO}$ and $M\Phi_{Tg}$ supports this possibility; in the absence of iPLA$_2$β, there is a reduced inflammatory state, which unmasks pathways leading to production of resolvin D2; whereas a heightened inflammatory status in $M\Phi_{Tg}$ mitigates such processes. Overall, our lipidomics analyses suggest a

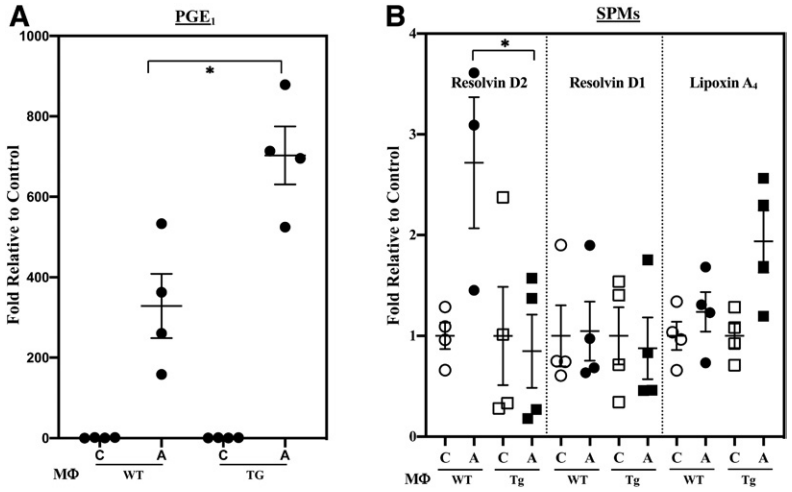

Fig. 9. Production of anti-inflammatory PGE_1 and SPMs $M\Phi_{WT}$ and $M\Phi_{Tg}$. Peritoneal macrophages isolated from 8-week-old WT and Tg mice were treated with vehicle [control (C)], IFNγ + LPS, or IL-4 and the media collected for lipidomics analyses. The data represent activated (A) fold-changes in lipids relative to C. Data are mean ± SEM determined from four independent experiments. A: PGE_1 ± IFNγ + LPS. Control (pmol lipid/$1e^{+06}$) $M\Phi_{WT}$ and $M\Phi_{Tg}$: 0.033 ± 0.011 and 0.017 ± 0.003. B: SPMs ± IL-4. Control (pmol lipid/$1e^{+06}$) $M\Phi_{WT}$ and $M\Phi_{Tg}$: resolvin D2, 0.561 ± 0.073 and 1.074 ± 0.524; resolvin D1, 0.134 ± 0.042 and 0.136 ± 0.039; lipoxin A_4, 0.050 ± 0.008 and 0.050 ± 0.006. *$M\Phi_{Tg}$ significantly different from $M\Phi_{WT}$, $P < 0.05$.

pro-inflammatory status in $M\Phi_{Tg}$ and, consistently, polarization of $M\Phi_{Tg}$ favored an M1 over M2 phenotype.

Examination of potential involvement of other PLA_2s expressed in macrophages revealed an absence in induction of $sPLA_2$ GV or $cPLA_2\alpha$ in activated $M\Phi_{Tg}$. Because $M\Phi_{Tg}$ exhibited more profound lipid changes with classical activation, we tested the impact of inhibiting $sPLA_2$s or $cPLA_2\alpha$ on the lipid profile under this condition. Production of eicosanoids by $M\Phi_{WT}$ or $M\Phi_{Tg}$ under basal or activated conditions were found to be similar following exposure to CAY 10502, which inhibits $cPLA_2\alpha$, or LY315920, which inhibits mGIB, mGIIA, mGIID, mGIIE, mGV, and mGX $sPLA_2$ (personal communication). In the presence of LY315920, basal production of pro-inflammatory PGs by $M\Phi_{Tg}$ was found to be higher relative to $M\Phi_{WT}$, most likely a reflection of modest decreases in their abundances in the WT group. Nevertheless, the inability of either CAY 10502 or LY315920 to mitigate the select lipid changes in $M\Phi_{Tg}$ relative to $M\Phi_{WT}$ suggests that neither $sPLA_2$s nor $cPLA_2\alpha$ contribute to the pro-inflammatory lipid profile in $M\Phi_{Tg}$ during the activated state during the time course of our studies. Additionally, expression of *ALOX-12* and *PTGS2* mRNA, which encode 12-LO and COX2 proteins, respectively, were similar in the $M\Phi_{WT}$ and $M\Phi_{Tg}$, suggesting that they likely are not responsible for the differences between the two groups.

These studies add to a growing body of literature indicating a role for $iPLA_2\beta$ in inflammatory disease, particularly in T1D. We previously reported that glucose-stimulated insulin secretion (GSIS) is accompanied by $iPLA_2\beta$-mediated hydrolysis of AA from β-cell membrane glycerophospholipids and that overexpression of $iPLA_2\beta$ leads to higher GSIS (6, 7, 9). As reported in those studies, the *RIP.iPLA$_2\beta$.Tg* mice exhibited lower circulating glucose levels and amplified GSIS insulin (43). Further, whereas survival of β-cells (INS-1 or in *RIP.iPLA$_2\beta$.Tg* islets) was unaffected by $iPLA_2\beta$ overexpression under basal conditions, ER stress and pro-inflammatory cytokines amplified apoptosis of the β-cells (44, 48, 61, 90–92). It is important to note that the impact of $iPLA_2\beta$ on insulin secretion is evident within 1 h of glucose stimulation and is not associated with an increase in $iPLA_2\beta$ expression. In contrast, its effect on β-cell survival is manifested after several hours of exposure to ER stressors or pro-inflammatory cytokines and is associated with induction of $iPLA_2\beta$ (44, 48, 61, 62, 90, 92, 93).

In this regard, it was intriguing to find that $iPLA_2\beta$ mRNA was modestly higher in $M\Phi_{Tg}$ relative to $M\Phi_{WT}$. However, this did not translate to greater protein expression or increased production of lipids by resting $M\Phi_{Tg}$. In contrast, classical activation led to significantly higher production of the select lipids by $M\Phi_{Tg}$, and this may be a consequence of increased availability of substrates derived through $iPLA_2\beta$-mediated hydrolysis of *sn*-2 fatty acyl substituents for metabolism by downstream enzymes. This is analogous to previous reports of minimal effects of higher $iPLA_2\beta$ expression in β-cells under basal conditions, but amplified in response to stress (43, 44), suggesting that the $iPLA_2\beta$ overexpressing β-cells are sensitized to respond to stimulation. Our current observations raise the possibility that there may be cross-talk between β-cells and

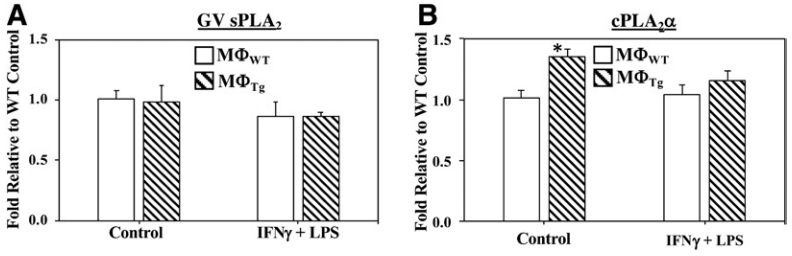

Fig. 10. Comparison of GV $sPLA_2$ and $cPLA_2\alpha$ mRNA in $M\Phi_{WT}$ and $M\Phi_{Tg}$. Peritoneal macrophages isolated from 8-week-old WT and Tg mice were treated with vehicle (Control) or IFNγ + LPS. The cells were harvested and processed for real-time qPCR analyses. A: *$sPLA_2$* GV (Control $M\Phi_{WT}$ $2^{-\Delta\Delta CT}$, 1.01 ± 0.06). B: *$cPLA_2\alpha$* (Control $M\Phi_{WT}$ $2^{-\Delta\Delta CT}$, 1.01 ± 0.07). Data are mean ± SEM of fold-change relative to control determined from four independent experiments. *$M\Phi_{Tg}$ significantly different from $M\Phi_{WT}$, $P < 0.01$.)

TABLE 4. Effects of $sPLA_2$ and $cPLA_2$ inhibition on basal eicosanoid production from $M\Phi_{WT}$ and $M\Phi_{Tg}$

	$M\Phi_{WT}$ (n = 4) (pmol lipid/1e^{+06})			$M\Phi_{Tg}$ (n = 3) (pmol lipid/1e^{+06})		
Lipid	DMSO	+$sPLA_2$ Inhibitor	+$cPLA_2$ Inhibitor	DMSO	+$sPLA_2$ Inhibitor	+$cPLA_2$ Inhibitor
6-Keto $PGF_1\alpha$	5.555 ± 0.585	4.775 ± 0.599	5.425 ± 1.082	9.418 ± 2.493	9.742 ± 1.732[a]	9.604 ± 3.708
TXB_2	4.619 ± 0.173	4.575 ± 0.190	4.696 ± 0.188	4.949 ± 0.108	4.892 ± 0.294	5.108 ± 0.593
PGE_2	2.343 ± 0.297	2.320 ± 0.406	3.944 ± 1.372	3.734 ± 1.053	5.347 ± 1.074[a]	8.549 ± 5.762
PGA_2	1.674 ± 0.114	1.550 ± 0.074	1.858 ± 0.207	1.850 ± 0.176	2.010 ± 0.143[a]	2.008 ± 0.322
PGD_2	0.395 ± 0.058	0.330 ± 0.046	0.419 ± 0.067	0.413 ± 0.027	0.507 ± 0.145	0.705 ± 0.137
$PGF_2\alpha$	0.638 ± 0.043	0.536 ± 0.022	0.579 ± 0.053	0.613 ± 0.021	0.649 ± 0.032[a]	00.685 ± 0.069
PGE_1	0.332 ± 0.059	0.288 ± 0.037	0.633 ± 0.250	0.532 ± 0.105	0.648 ± 0.167	1.239 ± 0.864
Resolvin D1	0.516 ± 0.012	0.509 ± 0.008	0.506 ± 0.012	0.520 ± 0.017	0.514 ± 0.009	0.495 ± 0.006
LTE_4	0.928 ± 0.107	0.959 ± 0.151	0.762 ± 0.072	12.560 ± 1.089	1.879 ± 0.285[a]	1.411 ± 0.600
(±)14,15-DHET	0.671 ± 0.018	0.639 ± 0.017	0.626 ± 0.021	0.664 ± 0.100	0.643 ± 0.026	0.678 ± 0.021
(±)11,12-DHET	0.761 ± 0.017	0.725 ± 0.016	0.757 ± 0.047	0.745 ± 0.010	0.729 ± 0.012	0.788 ± 0.027
(±)8,9-DHET	0.717 ± 0.052	0.655 ± 0.015	0.692 ± 0.052	0.697 ± 0.048	0.713 ± 0.021	0.881 ± 0.102
(±)14(15)-EET	0.458 ± 0.028	0.403 ± 0.009	0.458 ± 0.024	0.479 ± 0.044	0.432 ± 0.026	0.468 ± 0.032
(±)8(9)-EET	0.044 ± 0.014	0.111 ± 0.059	0.123 ± 0.077	0.182 ± 0.067	0.132 ± 0.073	0.048 ± 0.007
20-HETE	48.113 ± 0.951	47.770 ± 1.245	46.796 ± 1.049	54.631 ± 5.502	52.000 ± 3.387	51.376 ± 2.587
15-HETE	8.658 ± 0.492	8.344 ± 0.194	9.514 ± 0.749	9.049 ± 0.390	8.850 ± 0.367	10.759 ± 1.188
12-HETE	26.115 ± 3.799	24.261 ± 1.304	30.636 ± 1.518	30.433 ± 3.028	27.678 ± 0.959	40.769 ± 5.260
5-HETE	15.490 ± 0.906	15.002 ± 0.897	16.287 ± 1.389	16.100 ± 2.337	15.301 ± 1.812	17.798 ± 1.123
EPA	110.120 ± 4.666	108.113 ± 5.052	108.650 ± 6.474	120.756 ± 4.953	116.367 ± 3.977	123.173 ± 3.299
DHA	541.748 ± 25.043	528.699 ± 24.293	531.345 ± 24.191	528.597 ± 16.190	535.621 ± 26.864	539.104 ± 25.425
AA	1,416.140 ± 136.869	1,346.699 ± 115.662	1,413.377 ± 126.250	1,431.009 ± 165.233	1,391.521 ± 170.268	1,547.321 ± 140.321
DHGLA	461.100 ± 37.288	438.201 ± 39.349	457.010 ± 33.448	472.864 ± 54.049	427.581 ± 46.155	486.472 ± 17.667

Media from $M\Phi_{WT}$ and $M\Phi_{Tg}$ treated with vehicle, $sPLA_2$ inhibitor (LY315920), or $cPLA_2$ inhibitor (CAY 10502) only were processed for lipidomics analyses. The data are mean ± SEM.

[a]Significantly different from WT-$sPLA_2$ inhibitor, $P < 0.05$.

macrophages in vivo, to the extent that $M\Phi_{Tg}$ are predisposed to exhibiting enhanced responses to classical activation leading to an inflammatory landscape. While transfer of stress-induced signals between cells of different types has been suggested (60, 94, 95), to our knowledge, this is the first demonstration of lipid signaling generated by β-cells having an impact on an immune cell that elicits inflammatory consequences.

While the present study did not discern the intercellular signaling molecules in *RIP.iPLA$_2$β.Tg* mice, it is likely that they are derived directly or indirectly through an increase in iDLs, as a consequence of increased $iPLA_2\beta$ expression. In support of this, recent studies reveal that inhibition of $iPLA_2\beta$ activity mitigates inflammatory processes in different cell systems (18, 78, 96–98), raising the possibility that bioactive lipids generated through β-cell-$iPLA_2\beta$ activity or

TABLE 5. Effects of $sPLA_2$ and $cPLA_2$ inhibition on eicosanoid production from classically activated $M\Phi_{WT}$ and $M\Phi_{Tg}$

	$M\Phi_{WT}$ (n = 4) (pmol lipid/1e^{+06})			$M\Phi_{Tg}$ (n = 3) (pmol lipid/1e^{+06})		
Lipid	IFNγ + LPS alone	+$sPLA_2$ Inhibitor	+$cPLA_2$ Inhibitor	IFNγ + LPS alone	+$sPLA_2$ Inhibitor	+$cPLA_2$ Inhibitor
6-keto $PGF_1\alpha$	9.561 ± 0.967	9.263 ± 2.300	10.615 ± 2.484	25.550 ± 5.683[a]	24.711 ± 6.504	30.651 ± 11.155
TXB_2	5.483 ± 0.119	5.465 ± 0.425	5.607 ± 0.793	7.213 ± 0.608[a]	6.680 ± 0.422	7.672 ± 1.082
PGE_2	12.345 ± 1.661	11.542 ± 2.797	18.140 ± 5.066	29.945 ± 5.518[a]	28.940 ± 7.541	43.413 ± 17.386
PGA_2	2.745 ± 0.263	2.521 ± 0410	3.436 ± 0.707	5.029 ± 0.923	4.798 ± 1.116	6.769 ± 2.360
PGD_2	0.406 ± 0.013	0.372 ± 0.027	0.469 ± 0.101	0.629 ± 0.177	0.688 ± 0.237	1.239 ± 0.386
$PGF_2\alpha$	0.659 ± 0.040	0.595 ± 0.060	0.665 ± 0.137	0.882 ± 0.105	0.865 ± 0.123	1.002 ± 0.226
PGE_1	1.862 ± 0.264	1.791 ± 0.509	3.129 ± 1.055	5.253 ± 0.949[a]	4.707 ± 1.301	7.204 ± 2.719
Resolvin D1	0.497 ± 0.020	0.497 ± 0.012	0.519 ± 0.025	0.519 ± 0.016	0.493 ± 0.006	0.513 ± 0.017
LTE_4	0.993 ± 0.182	0.663 ± 0.170	0.631 ± 0.165	1.544 ± 0.471	1.555 ± 0.135*	0.776 ± 0.190
(±)14,15-DHET	0.652 ± 0.022	0.668 ± 0.044	0.602 ± 0.049	0.701 ± 0.033	0.700 ± 0.030	0.693 ± 0.030
(±)11,12-DHET	0.783 ± 0.062	0.792 ± 0.007	0.841 ± 0.057	0.823 ± 0.037	0.852 ± 0.015	0.865 ± 0.037
(±)8,9-DHET	0.683 ± 0.016	0.669 ± 0.049	0.833 ± 0.180	0.716 ± 0.036	0.906 ± 0.132	0.934 ± 0.094
(±)14(15)-EET	0.473 ± 0.012	0.440 ± 0.019	0.525 ± 0.027	0.446 ± 0.019	0.464 ± 0.035	0.573 ± 0.050
(±)8(9)-EET	0.127 ± 0.089	0.063 ± 0.011	0.031 ± 0.009	0.217 ± 0.086	0.049 ± 0.011	0.046 ± 0.009
20-HETE	49.441 ± 1.344	48.211 ± 0.504	51.483 ± 1.518	48.650 ± 3.136	49.563 ± 1.295	53.640 ± 3.342
15-HETE	10.040 ± 0.608	9.840 ± 0.902	10.632 ± 1.832	13.091 ± 1.920	12.933 ± 1.949	14.962 ± 2.682
12-HETE	27.123 ± 2.916	25.808 ± 1.084	30.599 ± 3.665	37.284 ± 8.799	40.913 ± 6.892	49.287 ± 11.085
5-HETE	14.827 ± 1.023	14.756 ± 0.983	15.383 ± 0.506	14.036 ± 0.558	14.717 ± 1.211	17.931 ± 1.451
EPA	97.624 ± 9.624	89.281 ± 6.085	87.666 ± 1.709	92.912 ± 4.441	92.378 ± 5.735	96.929 ± 5.827
DHA	531.386 ± 27.303	512.364 ± 27.212	497.151 ± 34.632	517.238 ± 20.479	497.449 ± 34.805	519.231 ± 29.269
AA	1,326.516 ± 36.127	1,276.119 ± 58.193	1,300.538 ± 27.380	1,241.023 ± 39.727	1,247.448 ± 62.748	1,557.577 ± 174.420
DHGLA	428.036 ± 32.703	395.946 ± 21.708	410.002 ± 20.994	401.953 ± 14.966	392.479 ± 31.565	482.797 ± 49.330

Media from $M\Phi_{WT}$ and $M\Phi_{Tg}$ treated with IFNγ + LPS ± $sPLA_2$ (LY315920) or $cPLA_2$ (CAY 10502) inhibitor were processed for lipidomics analyses. The data are mean ± SEM.

[a]Significantly different from WT-FNγ + LPS, $P < 0.05$.

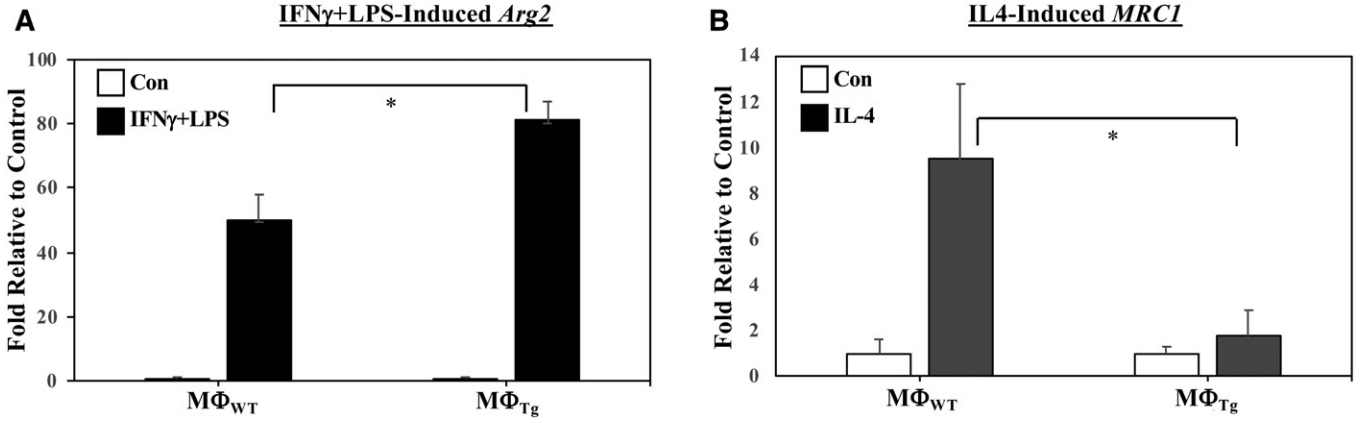

Fig. 11. Induction of M1 (*Arg2*) and M2 (*MRC1*) markers in $M\Phi_{WT}$ and $M\Phi_{Tg}$. Peritoneal macrophages isolated from 8-week-old WT and Tg mice were treated with vehicle [control (Con)], IFNγ + LPS, or IL-4. The cells were harvested and processed for real-time qPCR analyses. A: *Arg2* (Control $M\Phi_{WT}$ and $M\Phi_{Tg}$ $2^{-\Delta\Delta CT}$, 2.21 ± 0.86 and 2.41 ± 0.39). B: *MRC1* (Control $M\Phi_{WT}$ and $M\Phi_{Tg}$ $2^{-\Delta\Delta CT}$, 4.81 ± 2.91 and 15.38 ± 4.28). Data are mean ± SEM of fold-change relative to Con determined from four independent experiments. *$M\Phi_{Tg}$ significantly different from $M\Phi_{WT}$, $P < 0.05$.

factors arising from the effects of such lipids may serve as potential candidate intercellular signals. For instance, insulin secretion from β-cells is accompanied by a parallel $iPLA_2\beta$-mediated hydrolysis of AA from β-cell membranes and generation of PGE_2, which is mitigated by selective inhibition of $iPLA_2\beta$ (7, 99). Mice with selective overexpression of $iPLA_2\beta$ in β- cells exhibit lower basal blood glucose (43). Further β-cells in these mice express higher pPERK and generate more ceramides under basal conditions (44). This leads to the possibility that circulating insulin, PGE_2 or other iDLs, ER stress factors, or ceramides originating from β-cells could prime macrophages to respond more robustly to classical activation. This is supported by the greater induction of *Arg2* and lower induction of *MRC1* in $M\Phi_{Tg}$, which sets the table for the onset and progression of an inflammatory state. Further detailed studies are needed to identify the specific signals from β-cells that affect macrophages and they are currently underway.

The importance of intercellular signaling originating from β-cells is realized in view of findings that β-cells in the diabetes-prone NOD mice express higher $iPLA_2\beta$ during the prediabetic phase relative to β-cells in spontaneous diabetes-resistant models (20). This early phase encompasses spontaneous evolution of inflammatory signaling leading to the onset of insulitis. Our findings offer the possibility that higher activation of $iPLA_2\beta$ in the β-cells of

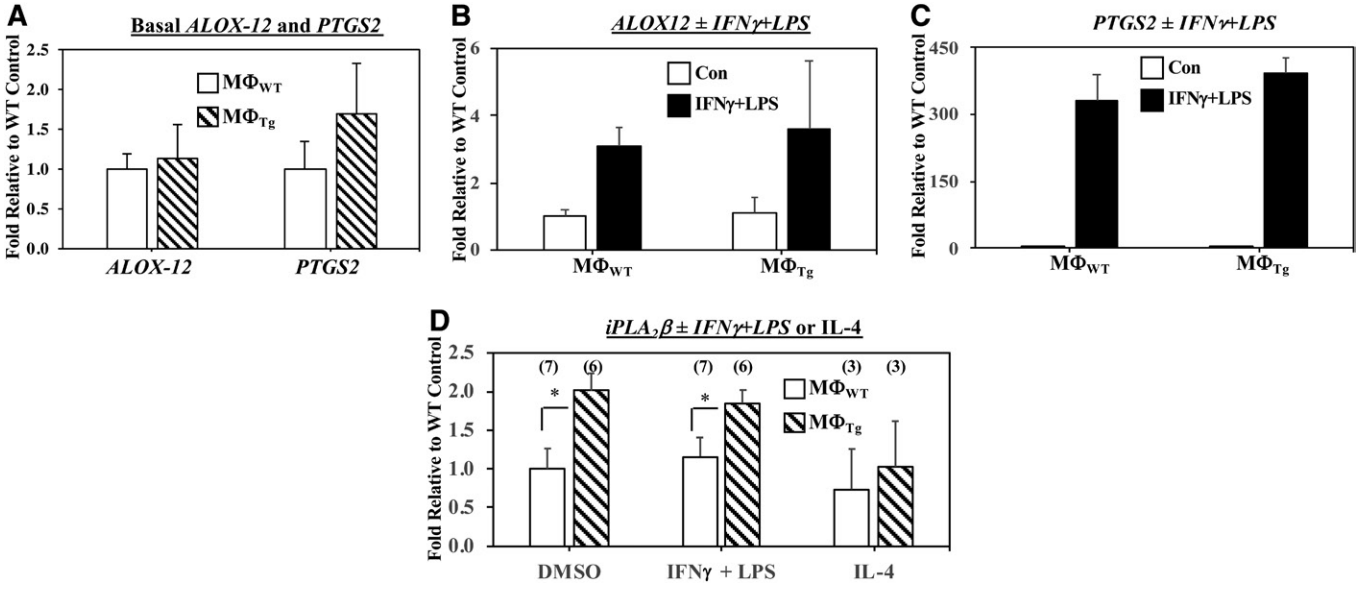

Fig. 12. Comparisons of PLA_2, ALOX-12, and PTGS2 mRNA in $M\Phi_{WT}$ and $M\Phi_{Tg}$. Peritoneal macrophages isolated from 8-week-old WT and Tg mice were treated with vehicle (Control) or activated with IFNγ + LPS or IL-4. The cells were harvested and processed for real-time qPCR analyses for *ALOX-12* (A, B) and *PGST2* (A, C) ± IFNγ + LPS, and *$iPLA_2\beta$* ± IFNγ + LPS or IL-4 (D). A: Control *ALOX-12* and *PTGS2* $2^{-\Delta\Delta CT}$, 6.46 ± 1.17 and 2.98 ± 1.04. B: Control $M\Phi_{WT}$ $2^{-\Delta\Delta CT}$, 6.46 ± 1.17. C: Control $M\Phi_{WT}$ $2^{-\Delta\Delta CT}$, 2.98 ± 1.04. D: Control $M\Phi_{WT}$ $2^{-\Delta\Delta CT}$, 1.01 ± 0.084. Data are mean ± SEM of fold-change relative to control determined from four independent experiments. *$M\Phi_{Tg}$ significantly different from $M\Phi_{WT}$, $P < 0.05$.

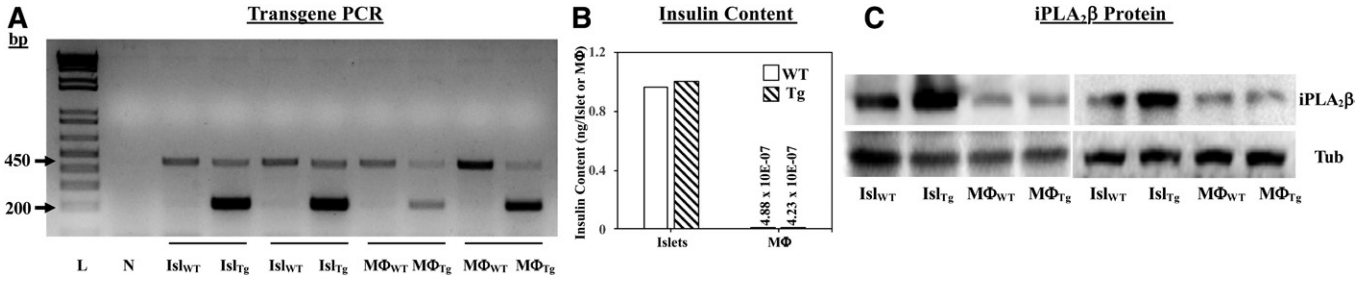

Fig. 13. Transgene verification. Pancreatic islets and peritoneal macrophages were isolated from 8-week-old WT and Tg mice for the following analyses: A: Transgene PCR. Analyses were performed using cDNA from WT or *RIP.iPLA$_2$β.TG* (Tg) mice, and primers that amplify sequence that either spans junction between iPLA$_2$β and globin. cDNA (200 bp product, lower band) or is within internal control *Fabpi* (450 bp product, upper band). Lane L, molecular weight ladder; lane N, control reaction without template. B: Insulin content was determined by ELISA using acid-extracted samples. C: iPLA$_2$β and tubulin (loading control) immunoblotting were performed using 30 μg protein. The data were obtained from two independent replicates.

NOD mice during this phase contributes signals that can be transmitted to infiltrating leukocytes to initiate immune responses that work in concert with events in the β-cells to amplify the onset and progression of inflammation that subsequently induces β-cell death and T1D. As discussed in a recent review (100), inflammation and β-cell dysfunction are also associated with the development of insulin resistance, and iPLA$_2$β has been implicated in this process as well, suggesting that signaling between β-cells and immune cells must also be considered as a contributor to the development of T2D.

In summary, our findings reveal that iPLA$_2$β modulates macrophage production of select lipids, which collectively are recognized to be associated with an enhanced inflammatory state. The selective nature of the lipid changes suggests that the impact of iPLA$_2$β is not broad but is specific to certain pathways that lead to the generation of such lipids. We find that induction of an M1 inflammatory macrophage phenotype is associated with increased production of iPLA$_2$β-derived pro-inflammatory lipids and that responses in macrophages can be modulated by iPLA$_2$β-derived signals of β-cell origin. These findings raise the importance of assessing more carefully the mechanisms governing modulation of the function of immune cells constituting an inflammatory landscape.

The authors would like to thank Dr. Jason W. Ashley and Dr. Robert N. Bone for their advice on macrophage assays and Dr. Gerard Lambeau for his advice on sPLA$_2$ inhibitors.

REFERENCES

1. Atkinson, M. A., and N. K. Maclaren. 1994. The pathogenesis of insulin-dependent diabetes mellitus. *N. Engl. J. Med.* **331:** 1428–1436.
2. Gilroy, D. W., J. Newson, P. Sawmynaden, D. A. Willoughby, and J. D. Croxtall. 2004. A novel role for phospholipase A$_2$ isoforms in the checkpoint control of acute inflammation. *FASEB J.* **18:** 489–498.
3. Khanapure, S. P., D. S. Garvey, D. R. Janero, and L. G. Letts. 2007. Eicosanoids in inflammation: biosynthesis, pharmacology, and therapeutic frontiers. *Curr. Top. Med. Chem.* **7:** 311–340.
4. Basu, S., A. Larsson, J. Vessby, B. Vessby, and C. Berne. 2005. Type 1 diabetes is associated with increased cyclooxygenase- and cytokine-mediated inflammation. *Diabetes Care.* **28:** 1371–1375.
5. Luo, P., and M. H. Wang. 2011. Eicosanoids, beta-cell function, and diabetes. *Prostaglandins Other Lipid Mediat.* **95:** 1–10.
6. Ramanadham, S., R. W. Gross, X. Han, and J. Turk. 1993. Inhibition of arachidonate release by secretagogue-stimulated pancreatic islets suppresses both insulin secretion and the rise in β-cell cytosolic calcium ion concentration. *Biochemistry.* **32:** 337–346.
7. Ramanadham, S., A. Bohrer, M. Mueller, P. Jett, R. W. Gross, and J. Turk. 1993. Mass spectrometric identification and quantitation of arachidonate-containing phospholipids in pancreatic islets: prominence of plasmenylethanolamine molecular species. *Biochemistry.* **32:** 5339–5351.
8. Ramanadham, S., R. Gross, and J. Turk. 1992. Arachidonic acid induces an increase in the cytosolic calcium concentration in single pancreatic islet beta cells. *Biochem. Biophys. Res. Commun.* **184:** 647–653.
9. Ramanadham, S., F-F. Hsu, A. Bohrer, Z. Ma, and J. Turk. 1999. Studies of the role of group VI phospholipase A$_2$ in fatty acid incorporation, phospholipid remodeling, lysophosphatidylcholine generation, and secretagogue-induced arachidonic acid release in pancreatic islets and insulinoma cells. *J. Biol. Chem.* **274:** 13915–13927.
10. Nowatzke, W., S. Ramanadham, Z. Ma, F. F. Hsu, A. Bohrer, and J. Turk. 1998. Mass spectrometric evidence that agents that cause loss of Ca^{2+} from intracellular compartments induce hydrolysis of arachidonic acid from pancreatic islet membrane phospholipids by a mechanism that does not require a rise in cytosolic Ca^{2+} concentration. *Endocrinology.* **139:** 4073–4085.
11. Ramanadham, S., H. Song, F. F. Hsu, S. Zhang, M. Crankshaw, G. A. Grant, C. B. Newgard, S. Bao, Z. Ma, and J. Turk. 2003. Pancreatic islets and insulinoma cells express a novel isoform of group VIA phospholipase A$_2$ (iPLA$_2$β) that participates in glucose-stimulated insulin secretion and is not produced by alternate splicing of the iPLA$_2$β transcript. *Biochemistry.* **42:** 13929–13940.
12. Ramanadham, S., M. J. Wolf, P. A. Jett, R. W. Gross, and J. Turk. 1994. Characterization of an ATP-stimulatable Ca^{2+}-independent phospholipase A$_2$ from clonal insulin-secreting HIT cells and rat pancreatic islets: a possible molecular component of the beta-cell fuel sensor. *Biochemistry.* **33:** 7442–7452.
13. Xie, L., X. Zhu, Y. Hu, T. Li, Y. Gao, Y. Shi, and S. Tang. 2008. Mitochondrial DNA oxidative damage triggering mitochondrial dysfunction and apoptosis in high glucose-induced HRECs. *Invest. Ophthalmol. Vis. Sci.* **49:** 4203–4209.
14. Rahnema, P., Y. Shimoni, and A. Nygren. 2011. Reduced conduction reserve in the diabetic rat heart: role of iPLA$_2$ activation in the response to ischemia. *Am. J. Physiol. Heart Circ. Physiol.* **300:** H326–H334.
15. Ayilavarapu, S., A. Kantarci, G. Fredman, O. Turkoglu, K. Omori, H. Liu, T. Iwata, M. Yagi, H. Hasturk, and T. E. Van Dyke. 2010. Diabetes-Induced oxidative stress is mediated by Ca^{2+}-independent phospholipase A$_2$ in neutrophils. *J. Immunol.* **184:** 1507–1515.
16. Gil-de-Gómez, L., A. M. Astudillo, C. Guijas, V. Magrioti, G. Kokotos, M. A. Balboa, and J. Balsinde. 2014. Cytosolic group IVA and calcium-independent group VIA phospholipase A$_2$s act on distinct phospholipid pools in zymosan-stimulated mouse peritoneal macrophages. *J. Immunol.* **192:** 752–762.

17. Lee, S. H., D. W. Park, S. C. Park, Y. K. Park, S. Y. Hong, J. R. Kim, C. H. Lee, and S. H. Baek. 2009. Calcium-independent phospholipase A_2beta-Akt signaling is involved in lipopolysaccharide-induced NADPH oxidase 1 expression and foam cell formation. *J. Immunol.* **183:** 7497–7504.
18. Tan, C., R. Day, S. Bao, J. Turk, and Q. D. Zhao. 2014. Group VIA phospholipase A_2 mediates enhanced macrophage migration in diabetes mellitus by increasing expression of nicotinamide adenine dinucleotide phosphate oxidase 4. *Arterioscler. Thromb. Vasc. Biol.* **34:** 768–778.
19. Bao, S., Y. Li, X. Lei, M. Wohltmann, W. Jin, A. Bohrer, C. F. Semenkovich, S. Ramanadham, I. Tabas, and J. Turk. 2007. Attenuated free cholesterol loading-induced apoptosis but preserved phospholipid composition of peritoneal macrophages from mice that do not express group VIA phospholipase A_2. *J. Biol. Chem.* **282:** 27100–27114.
20. Bone, R. N., Y. Gai, V. Magrioti, M. G. Kokotou, T. Ali, X. Lei, H. M. Tse, G. Kokotos, and S. Ramanadham. 2015. Inhibition of Ca^{2+}-independent phospholipase $A_2\beta$ (iPLA$_2\beta$) ameliorates islet infiltration and incidence of diabetes in NOD mice. *Diabetes.* **64:** 541–554.
21. Liu, S., Z. Xie, Q. Zhao, H. Pang, J. Turk, L. Calderon, W. Su, G. Zhao, H. Xu, M. C. Gong, et al. 2012. Smooth muscle-specific expression of calcium-independent phospholipase $A_2\beta$ (iPLA$_2\beta$) participates in the initiation and early progression of vascular inflammation and neointima formation. *J. Biol. Chem.* **287:** 24739–24753.
22. Ming, W. J., L. Bersani, and A. Mantovani. 1987. Tumor necrosis factor is chemotactic for monocytes and polymorphonuclear leukocytes. *J. Immunol.* **138:** 1469–1474.
23. Held, W., H. R. MacDonald, I. L. Weissman, M. W. Hess, and C. Mueller. 1990. Genes encoding tumor necrosis factor alpha and granzyme A are expressed during development of autoimmune diabetes. *Proc. Natl. Acad. Sci. USA.* **87:** 2239–2243.
24. Herrera, P. L., D. M. Harlan, and P. Vassalli. 2000. A mouse CD8 T cell-mediated acute autoimmune diabetes independent of the perforin and Fas cytotoxic pathways: possible role of membrane TNF. *Proc. Natl. Acad. Sci. USA.* **97:** 279–284.
25. Lauber, K., E. Bohn, S. M. Krober, Y. J. Xiao, S. G. Blumenthal, R. K. Lindemann, P. Marini, C. Wiedig, A. Zobywalski, S. Baksh, et al. 2003. Apoptotic cells induce migration of phagocytes via caspase-3-mediated release of a lipid attraction signal. *Cell.* **113:** 717–730.
26. Zhao, X., D. Wang, Z. Zhao, Y. Xiao, S. Sengupta, Y. Xiao, R. Zhang, K. Lauber, S. Wesselborg, L. Feng, et al. 2006. Caspase-3-dependent activation of calcium-independent phospholipase A_2 enhances cell migration in non-apoptotic ovarian cancer cells. *J. Biol. Chem.* **281:** 29357–29368.
27. Mishra, R. S., K. A. Carnevale, and M. K. Cathcart. 2008. iPLA$_2$beta: front and center in human monocyte chemotaxis to MCP-1. *J. Exp. Med.* **205:** 347–359.
28. Kalyvas, A., C. Baskakis, V. Magrioti, V. Constantinou-Kokotou, D. Stephens, R. Lopez-Vales, J. Q. Lu, V. W. Yong, E. A. Dennis, G. Kokotos, et al. 2009. Differing roles for members of the phospholipase A_2 superfamily in experimental autoimmune encephalomyelitis. *Brain.* **132:** 1221–1235.
29. Li, H., Z. Zhao, C. Antalis, Z. Zhao, R. Emerson, G. Wei, S. Zhang, Z. Y. Zhang, and Y. Xu. 2011. Combination therapy of an inhibitor of group VIA phospholipase A_2 with paclitaxel is highly effective in blocking ovarian cancer development. *Am. J. Pathol.* **179:** 452–461.
30. McHowat, J., G. Gullickson, R. G. Hoover, J. Sharma, J. Turk, and J. Kornbluth. 2011. Platelet-activating factor and metastasis: calcium-independent phospholipase A_2beta deficiency protects against breast cancer metastasis to the lung. *Am. J. Physiol. Cell Physiol.* **300:** C825–C832.
31. Nicotera, T. M., D. P. Schuster, M. Bourhim, K. Chadha, G. Klaich, and D. A. Corral. 2009. Regulation of PSA secretion and survival signaling by calcium-independent phopholipase $A_2\beta$ in prostate cancer cells. *Prostate.* **69:** 1270–1280.
32. Scuderi, M. R., C. D. Anfuso, G. Lupo, C. Motta, L. Romeo, L. Guerra, A. Cappellani, N. Ragusa, G. Cantarella, and M. Alberghina. 2008. Expression of Ca^{2+}-independent and Ca^{2+}-dependent phospholipases A_2 and cyclooxygenases in human melanocytes and malignant melanoma cell lines. *Biochim. Biophys. Acta.* **1781:** 635–642.
33. Padgett, L. E., K. A. Broniowska, P. A. Hansen, J. A. Corbett, and H. M. Tse. 2013. The role of reactive oxygen species and proinflammatory cytokines in type 1 diabetes pathogenesis. *Ann. N. Y. Acad. Sci.* **1281:** 16–35.
34. Mantovani, A., A. Sica, S. Sozzani, P. Allavena, A. Vecchi, and M. Locati. 2004. The chemokine system in diverse forms of macrophage activation and polarization. *Trends Immunol.* **25:** 677–686.
35. Martinez, F. O., and S. Gordon. 2014. The M1 and M2 paradigm of macrophage activation: time for reassessment. *F1000Prime Rep.* **6:** 13.
36. Calderon, B., A. Suri, and E. R. Unanue. 2006. In $CD4^+$ T-cell-induced diabetes, macrophages are the final effector cells that mediate islet beta-cell killing: studies from an acute model. *Am. J. Pathol.* **169:** 2137–2147.
37. Parsa, R., P. Andresen, A. Gillett, S. Mia, X. M. Zhang, S. Mayans, D. Holmberg, and R. A. Harris. 2012. Adoptive transfer of immunomodulatory M2 macrophages prevents type 1 diabetes in NOD mice. *Diabetes.* **61:** 2881–2892.
38. Guimaraes, J. P. T., L. R. Filgueiras, J. O. Martins, and S. Jancar. 2019. Leukotriene involvement in the insulin receptor pathway and macrophage profiles in muscles from type 1 diabetic mice. *Mediators Inflamm.* **2019:** 4596127.
39. Duan, L., H. Gan, J. Arm, and H. G. Remold. 2001. Cytosolic phospholipase A_2 participates with TNF-alpha in the induction of apoptosis of human macrophages infected with Mycobacterium tuberculosis H37Ra. *J. Immunol.* **166:** 7469–7476.
40. Nikolic, D. M., M. C. Gong, J. Turk, and S. R. Post. 2007. Class A scavenger receptor-mediated macrophage adhesion requires coupling of calcium-independent phospholipase A_2 and 12/15-lipoxygenase to Rac and Cdc42 activation. *J. Biol. Chem.* **282:** 33405–33411.
41. Zaitseva, L., M. Vaisburd, G. Shaposhnikova, and E. Mysyakin. 2000. Role of eicosanoids in regulation of macrophage phagocytic functions by platelet-activating factor during endotoxic shock. *Bull. Exp. Biol. Med.* **130:** 879–881.
42. Ashley, J. W., W. D. Hancock, A. J. Nelson, R. N. Bone, H. M. Tse, M. Wohltmann, J. Turk, and S. Ramanadham. 2016. Polarization of macrophages toward M2 phenotype is favored by reduction in iPLA$_2\beta$ (Group VIA Phospholipase A_2). *J. Biol. Chem.* **291:** 23268–23281.
43. Bao, S., D. A. Jacobson, M. Wohltmann, A. Bohrer, W. Jin, L. H. Philipson, and J. Turk. 2008. Glucose homeostasis, insulin secretion, and islet phospholipids in mice that overexpress iPLA$_2\beta$ in pancreatic β-cells and in iPLA2beta-null mice. *Am. J. Physiol. Endocrinol. Metab.* **294:** E217–E229.
44. Lei, X., R. N. Bone, T. Ali, M. Wohltmann, Y. Gai, K. J. Goodwin, A. E. Bohrer, J. Turk, and S. Ramanadham. 2013. Genetic modulation of islet β-cell iPLA$_2\beta$ expression provides evidence for its impact on β-cell apoptosis and autophagy. *Islets.* **5:** 29–44.
45. Bao, S., D. J. Miller, Z. Ma, M. Wohltmann, G. Eng, S. Ramanadham, K. Moley, and J. Turk. 2004. Male mice that do not express group VIA phospholipase A_2 produce spermatozoa with impaired motility and have greatly reduced fertility. *J. Biol. Chem.* **279:** 38194–38200.
46. Blaho, V. A., M. W. Buczynski, C. R. Brown, and E. A. Dennis. 2009. Lipidomic analysis of dynamic eicosanoid responses during the induction and resolution of Lyme arthritis. *J. Biol. Chem.* **284:** 21599–21612.
47. Simanshu, D. K., R. K. Kamlekar, D. S. Wijesinghe, X. Zou, X. Zhai, S. K. Mishra, J. G. Molotkovsky, L. Malinina, E. H. Hinchcliffe, C. E. Chalfant, et al. 2013. Non-vesicular trafficking by a ceramide-1-phosphate transfer protein regulates eicosanoids. *Nature.* **500:** 463–467.
48. Lei, X., R. N. Bone, T. Ali, S. Zhang, A. Bohrer, H. M. Tse, K. R. Bidasee, and S. Ramanadham. 2014. Evidence of contribution of iPLA$_2\beta$-mediated events during islet beta-cell apoptosis due to proinflammatory cytokines suggests a role for iPLA$_2\beta$ in T1D development. *Endocrinology.* **155:** 3352–3364.
49. Ramanadham, S., F. F. Hsu, A. Bohrer, W. Nowatzke, Z. Ma, and J. Turk. 1998. Electrospray ionization mass spectrometric analyses of phospholipids from rat and human pancreatic islets and subcellular membranes: comparison to other tissues and implications for membrane fusion in insulin exocytosis. *Biochemistry.* **37:** 4553–4567.
50. Zhang, G., S. Kodani, and B. D. Hammock. 2014. Stabilized epoxygenated fatty acids regulate inflammation, pain, angiogenesis and cancer. *Prog. Lipid Res.* **53:** 108–123.
51. Balboa, M. A., J. Balsinde, M. V. Winstead, J. A. Tischfield, and E. A. Dennis. 1996. Novel group V phospholipase A_2 involved in

arachidonic acid mobilization in murine P388D1 macrophages. *J. Biol. Chem.* **271:** 32381–32384.
52. Morioka, Y., A. Saiga, Y. Yokota, N. Suzuki, M. Ikeda, T. Ono, K. Nakano, N. Fujii, J. Ishizaki, H. Arita, et al. 2000. Mouse group X secretory phospholipase A_2 induces a potent release of arachidonic acid from spleen cells and acts as a ligand for the phospholipase A_2 receptor. *Arch. Biochem. Biophys.* **381:** 31–42.
53. Koratkar, R., E. Pequignot, W. W. Hauck, and L. D. Siracusa. 2002. The CAST/Ei strain confers significant protection against Apc(Min) intestinal polyps, independent of the resistant modifier of Min 1 (Mom1) locus. *Cancer Res.* **62:** 5413–5417.
54. MacPhee, M., K. P. Chepenik, R. A. Liddell, K. K. Nelson, L. D. Siracusa, and A. M. Buchberg. 1995. The secretory phospholipase A_2 gene is a candidate for the Mom1 locus, a major modifier of ApcMin-induced intestinal neoplasia. *Cell.* **81:** 957–966.
55. Markova, M., R. A. Koratkar, K. A. Silverman, V. E. Sollars, M. MacPhee-Pellini, R. Walters, J. P. Palazzo, A. M. Buchberg, L. D. Siracusa, and S. A. Farber. 2005. Diversity in secreted PLA_2-IIA activity among inbred mouse strains that are resistant or susceptible to Apc Min/+ tumorigenesis. *Oncogene.* **24:** 6450–6458.
56. Triggiani, M., F. Granata, G. Giannattasio, and G. Marone. 2005. Secretory phospholipases A_2 in inflammatory and allergic diseases: not just enzymes. *J. Allergy Clin. Immunol.* **116:** 1000–1006.
57. Smart, B. P., R. C. Oslund, L. A. Walsh, and M. H. Gelb. 2006. The first potent inhibitor of mammalian group X secreted phospholipase A_2: elucidation of sites for enhanced binding. *J. Med. Chem.* **49:** 2858–2860.
58. Barnett, J. M., G. W. McCollum, and J. S. Penn. 2010. Role of cytosolic phospholipase A_2 in retinal neovascularization. *Invest. Ophthalmol. Vis. Sci.* **51:** 1136–1142.
59. Hanna, V. S., and E. A. A. Hafez. 2018. Synopsis of arachidonic acid metabolism: A review. *J. Adv. Res.* **11:** 23–32.
60. Umamaheswaran, S., S. K. Dasari, P. Yang, S. K. Lutgendorf, and A. K. Sood. 2018. Stress, inflammation, and eicosanoids: an emerging perspective. *Cancer Metastasis Rev.* **37:** 203–211.
61. Lei, X., S. Zhang, S. E. Barbour, A. Bohrer, E. L. Ford, A. Koizumi, F. R. Papa, and S. Ramanadham. 2010. Spontaneous development of endoplasmic reticulum stress that can lead to diabetes mellitus is associated with higher calcium-independent phospholipase A_2 expression: a role for regulation by SREBP-1. *J. Biol. Chem.* **285:** 6693–6705.
62. Lei, X., S. Zhang, A. Bohrer, S. E. Barbour, and S. Ramanadham. 2012. Role of calcium-independent phospholipase A_2beta in human pancreatic islet beta-cell apoptosis. *Am. J. Physiol. Endocrinol. Metab.* **303:** E1386–E1395.
63. Abdulkhaleq, L. A., M. A. Assi, R. Abdullah, M. Zamri-Saad, Y. H. Taufiq-Yap, and M. N. M. Hezmee. 2018. The crucial roles of inflammatory mediators in inflammation: a review. *Vet. World.* **11:** 627–635.
64. Tessaro, F. H., T. S. Ayala, and J. O. Martins. 2015. Lipid mediators are critical in resolving inflammation: a review of the emerging roles of eicosanoids in diabetes mellitus. *BioMed Res. Int.* **2015:** 568408.
65. Kühn, H., and V. B. O'Donnell. 2006. Inflammation and immune regulation by 12/15-lipoxygenases. *Prog. Lipid Res.* **45:** 334–356.
66. Issan, Y., E. Hochhauser, A. Guo, K. H. Gotlinger, R. Kornowski, D. Leshem-Lev, E. Lev, E. Porat, E. Snir, C. I. Thompson, et al. 2013. Elevated level of pro-inflammatory eicosanoids and EPC dysfunction in diabetic patients with cardiac ischemia. *Prostaglandins Other Lipid Mediat.* **100–101:** 15–21.
67. Hooper, K. M., W. Kong, and D. Ganea. 2017. Prostaglandin E_2 inhibits Tr1 cell differentiation through suppression of c-Maf. *PLoS One.* **12:** e0179184.
68. Hooper, K. M., J. H. Yen, W. Kong, K. M. Rahbari, P. C. Kuo, A. M. Gamero, and D. Ganea. 2017. Prostaglandin E_2 Inhibition of IL-27 production in murine dendritic cells: a novel mechanism that involves IRF1. *J. Immunol.* **198:** 1521–1530.
69. Aoki, T., J. Frosen, M. Fukuda, K. Bando, G. Shioi, K. Tsuji, E. Ollikainen, K. Nozaki, J. Laakkonen, and S. Narumiya. 2017. Prostaglandin E_2-EP2-NF-kappaB signaling in macrophages as a potential therapeutic target for intracranial aneurysms. *Sci. Signal.* **10:** eaah6037.
70. Li, H., H. Y. Chen, W. X. Liu, X. X. Jia, J. G. Zhang, C. L. Ma, X. J. Zhang, F. Yu, and B. Cong. 2017. Prostaglandin E_2 restrains human Treg cell differentiation via E prostanoid receptor 2-protein kinase A signaling. *Immunol. Lett.* **191:** 63–72.
71. Ganapathy, V., T. Gurlo, H. O. Jarstadmarken, and H. von Grafenstein. 2000. Regulation of TCR-induced IFN-gamma release from islet-reactive non-obese diabetic $CD8^+$ T cells by prostaglandin E_2 receptor signaling. *Int. Immunol.* **12:** 851–860.
72. Ling, J. J., Y. J. Sun, D. Y. Zhu, Q. Chen, and X. Han. 2005. Potential role of NO in modulation of COX-2 expression and PGE_2 production in pancreatic beta-cells. *Acta Biochim. Biophys. Sin. (Shanghai).* **37:** 139–146.
73. Boizel, R., G. Bruttmann, P. Y. Benhamou, S. Halimi, and F. Stanke-Labesque. 2010. Regulation of oxidative stress and inflammation by glycaemic control: evidence for reversible activation of the 5-lipoxygenase pathway in type 1, but not in type 2 diabetes. *Diabetologia.* **53:** 2068–2070.
74. Chakrabarti, S. K., B. K. Cole, Y. Wen, S. R. Keller, and J. L. Nadler. 2009. 12/15-lipoxygenase products induce inflammation and impair insulin signaling in 3T3-L1 adipocytes. *Obesity (Silver Spring).* **17:** 1657–1663.
75. Imai, Y., A. D. Dobrian, M. A. Morris, D. A. Taylor-Fishwick, and J. L. Nadler. 2016. Lipids and immunoinflammatory pathways of beta cell destruction. *Diabetologia.* **59:** 673–678.
76. Huang, H., J. Weng, and M. H. Wang. 2016. EETs/sEH in diabetes and obesity-induced cardiovascular diseases. *Prostaglandins Other Lipid Mediat.* **125:** 80–89.
77. Jouihan, S. A., K. L. Zuloaga, W. Zhang, R. E. Shangraw, S. M. Krasnow, D. L. Marks, and N. J. Alkayed. 2013. Role of soluble epoxide hydrolase in exacerbation of stroke by streptozotocin-induced type 1 diabetes mellitus. *J. Cereb. Blood Flow Metab.* **33:** 1650–1656.
78. Luther, J. M., and N. J. Brown. 2016. Epoxyeicosatrienoic acids and glucose homeostasis in mice and men. *Prostaglandins Other Lipid Mediat.* **125:** 2–7.
79. Rodriguez, M., and M. Clare-Salzler. 2006. Eicosanoid imbalance in the NOD mouse is related to a dysregulation in soluble epoxide hydrolase and 15-PGDH expression. *Ann. N. Y. Acad. Sci.* **1079:** 130–134.
80. Gezginci-Oktayoglu, S., N. Orhan, and S. Bolkent. 2016. Prostaglandin-E_1 has a protective effect on renal ischemia/reperfusion-induced oxidative stress and inflammation mediated gastric damage in rats. *Int. Immunopharmacol.* **36:** 142–150.
81. Gundala, N. K. V., V. G. M. Naidu, and U. N. Das. 2018. Amelioration of streptozotocin-induced type 2 diabetes mellitus in Wistar rats by arachidonic acid. *Biochem. Biophys. Res. Commun.* **496:** 105–113.
82. Serhan, C. N., and B. D. Levy. 2018. Resolvins in inflammation: emergence of the pro-resolving superfamily of mediators. *J. Clin. Invest.* **128:** 2657–2669.
83. Norris, P. C., and E. A. Dennis. 2014. A lipidomic perspective on inflammatory macrophage eicosanoid signaling. *Adv. Biol. Regul.* **54:** 99–110.
84. Mouchlis, V. D., Y. Chen, J. A. McCammon, and E. A. Dennis. 2018. Membrane allostery and unique hydrophobic sites promote enzyme substrate specificity. *J. Am. Chem. Soc.* **140:** 3285–3291.
85. Triggiani, M., F. Granata, A. Oriente, V. De Marino, M. Gentile, C. Calabrese, C. Palumbo, and G. Marone. 2000. Secretory phospholipases A_2 induce beta-glucuronidase release and IL-6 production from human lung macrophages. *J. Immunol.* **164:** 4908–4915.
86. Ruipérez, V., J. Casas, M. A. Balboa, and J. Balsinde. 2007. Group V phospholipase A_2-derived lysophosphatidylcholine mediates cyclooxygenase-2 induction in lipopolysaccharide-stimulated macrophages. *J. Immunol.* **179:** 631–638.
87. Fantone, J. C., W. A. Marasco, L. J. Elgas, and P. A. Ward. 1983. Anti-inflammatory effects of prostaglandin E_1: in vivo modulation of the formyl peptide chemotactic receptor on the rat neutrophil. *J. Immunol.* **130:** 1495–1497.
88. Basselin, M., A. O. Rosa, E. Ramadan, Y. Cheon, L. Chang, M. Chen, D. Greenstein, M. Wohltmann, J. Turk, and S. I. Rapoport. 2010. Imaging decreased brain docosahexaenoic acid metabolism and signaling in $iPLA_2$beta (VIA)-deficient mice. *J. Lipid Res.* **51:** 3166–3173.
89. Cheon, Y., H. W. Kim, M. Igarashi, H. R. Modi, L. Chang, K. Ma, D. Greenstein, M. Wohltmann, J. Turk, S. I. Rapoport, et al. 2012. Disturbed brain phospholipid and docosahexaenoic acid metabolism in calcium-independent phospholipase A_2-VIA ($iPLA_2\beta$)-knockout mice. *Biochim. Biophys. Acta.* **1821:** 1278–1286.
90. Lei, X., S. Zhang, A. Bohrer, and S. Ramanadham. 2008. Calcium-independent phospholipase A_2 ($iPLA_2\beta$)-mediated ceramide generation plays a key role in the cross-talk between the endoplasmic reticulum (ER) and mitochondria during ER stress-induced insulin-secreting cell apoptosis. *J. Biol. Chem.* **283:** 34819–34832.

91. Lei, X., S. Zhang, B. Emani, S. E. Barbour, and S. Ramanadham. 2010. A link between endoplasmic reticulum stress-induced beta-cell apoptosis and the group VIA Ca^{2+}-independent phospholipase A_2 (iPLA$_2$β). *Diabetes Obes. Metab.* **12 (Suppl. 2):** 93–98.
92. Ramanadham, S., F. F. Hsu, S. Zhang, C. Jin, A. Bohrer, H. Song, S. Bao, Z. Ma, and J. Turk. 2004. Apoptosis of insulin-secreting cells induced by endoplasmic reticulum stress is amplified by overexpression of group VIA calcium-independent phospholipase A_2 (iPLA$_2$β) and suppressed by inhibition of iPLA$_2$β. *Biochemistry.* **43:** 918–930.
93. Lei, X., S. Zhang, A. Bohrer, S. Bao, H. Song, and S. Ramanadham. 2007. The group VIA calcium-independent phospholipase A_2 participates in ER stress-induced INS-1 insulinoma cell apoptosis by promoting ceramide generation via hydrolysis of sphingomyelins by neutral sphingomyelinase. *Biochemistry.* **46:** 10170–10185.
94. Papa, F. R. 2012. Endoplasmic reticulum stress, pancreatic beta-cell degeneration, and diabetes. *Cold Spring Harb. Perspect. Med.* **2:** a007666.
95. Shore, G. C., F. R. Papa, and S. A. Oakes. 2011. Signaling cell death from the endoplasmic reticulum stress response. *Curr. Opin. Cell Biol.* **23:** 143–149.
96. Amati, A. L., A. Zakrzewicz, R. Siebers, S. Wilker, S. Heldmann, D. Zakrzewicz, A. Hecker, J. M. McIntosh, W. Padberg, and V. Grau. 2017. Chemokines (CCL3, CCL4, and CCL5) inhibit ATP-induced release of IL-1beta by monocytic cells. *Mediators Inflamm.* **2017:** 1434872.
97. Lee, J. G., E. J. Lim, D. W. Park, S. H. Lee, J. R. Kim, and S. H. Baek. 2008. A combination of Lox-1 and Nox1 regulates TLR9-mediated foam cell formation. *Cell. Signal.* **20:** 2266–2275.
98. Schenten, V., S. Brechard, S. Plancon, C. Melchior, J. P. Frippiat, and E. J. Tschirhart. 2010. iPLA$_2$, a novel determinant in Ca^{2+}- and phosphorylation-dependent S100A8/A9 regulated NOX2 activity. *Biochim. Biophys. Acta.* **1803:** 840–847.
99. Ramanadham, S., A. Bohrer, R. W. Gross, and J. Turk. 1993. Mass spectrometric characterization of arachidonate-containing plasmalogens in human pancreatic islets and in rat islet β-cells and subcellular membranes. *Biochemistry.* **32:** 13499–13509.
100. Turk, J., T. D. White, A. J. Nelson, X. Lei, and S. Ramanadham. 2019. iPLA2β and its role in male fertility, neurological disorders, metabolic disorders, and inflammation. *Biochim. Biophys. Acta Mol. Cell Biol. Lipids.* **1864:** 846–860.
101. Eerola, L. I., F. Surrel, T. J. Nevalainen, M. H. Gelb, G. Lambeau, and V. J. Laine. 2006. Analysis of expression of secreted phospholipases A_2 in mouse tissues at protein and mRNA levels. *Biochim. Biophys. Acta.* **1761:** 745–756.